Random perfect lattices and the sphere packing problem

A. Andreanov[1] and A. Scardicchio[1,2]
[1]*Abdus Salam ICTP, Strada Costiera 11, 34151, Trieste, Italy*
[2]*INFN, Sezione di Trieste, via Valerio 2, 34127 Trieste, Italy*
(Received 31 July 2012; published 11 October 2012)

Motivated by the search for best lattice sphere packings in Euclidean spaces of large dimensions we study randomly generated perfect lattices in moderately large dimensions (up to $d = 19$ included). Perfect lattices are relevant in the solution of the problem of lattice sphere packing, because the best lattice packing is a perfect lattice and because they can be generated easily. Their number, however, grows superexponentially with the dimension, so to get an idea of their properties we propose to study a randomized version of the generating algorithm and to define a random ensemble with an effective temperature in a way reminiscent of a Monte Carlo simulation. We therefore study the distribution of packing fractions and kissing numbers of these ensembles and show how as the temperature is decreased the best known packers are easily recovered. We find that, even at infinite temperature, the typical perfect lattices are considerably denser than known families (like A_d and D_d), and we propose two hypotheses between which we cannot distinguish in this paper: one in which they improve the Minkowsky bound $\phi \sim 2^{-(0.84\pm0.06)d}$, and a competitor in which their packing fraction decreases superexponentially, namely, $\phi \sim d^{-ad}$ but with a very small coefficient $a = 0.06 \pm 0.04$. We also find properties of the random walk which are suggestive of a glassy system already for moderately small dimensions. We also analyze local structure of network of perfect lattices conjecturing that this is a scale-free network in all dimensions with constant scaling exponent 2.6 ± 0.1.

DOI: 10.1103/PhysRevE.86.041117 PACS number(s): 05.20.−y, 61.50.Ah

I. INTRODUCTION

Sphere packing is a classic problem with many connections to pure and applied mathematics (number theory and geometry [1]), communication theory [2], and physics [3]. The statement of the problem is very simple: Given an Euclidean space of dimension d what is the densest spatial arrangement of impenetrable spheres? In a more formal way one seeks to find a maximum over all packings:

$$\phi_{\text{best}}(d) = \max_{\mathcal{P}\in S} \phi(\mathcal{P}).$$

Here $\mathcal{P}$ is a packing of spheres (an allowed configuration of the impenetrable spheres), S is the set of all packings, and $\phi(\mathcal{P})$ is the fraction of space covered by the packing $\mathcal{P}$.

As is often the case with problems related to number theory, the simplest questions do not have simple answers. Despite over 200 years of research the problem has been solved only for $d = 2$ [4] and $d = 3$ [5] (the famous Kepler conjecture). The latter case has been proved only about 15 years ago and required a substantial amount of computer work. Although good and very good candidates for the best packings have been identified in higher dimensions (namely, $\lesssim 30$) our knowledge deteriorates quickly as dimensions become really high, say, of order 10^3, where the problem becomes of interest to communication theory.

One the greatest challenges in the sphere packing problem is that no universal behavior is identifiable. Every dimension seems to be peculiar, with some dimensions being very special, like 8,12,24. In the generic case there is no restriction on packings: They can be of any nature, ordered (crystalline breaking of translational symmetry), or even disordered. For relatively low dimensions, $d \leqslant 9$, the best (known) packings are all lattice packings, that is, packings where spheres are placed at the vertices of a certain Bravais lattice (one particle per unit cell of the lattice). In $d = 10$ for the first time, the best known packing is generated by a non-Bravais lattice [1]. Some recent works [6,7] conjecture that in high enough dimensions completely disordered packings might win over regular ones.

To understand the degree of difficulty of the problem it is sufficient to mention that even finding good upper bounds on best packing fractions uniformly valid for all dimensions have resisted all attacks so far. The 100-year-old lower bound by Minkowsky received only linear improvements until today, and an exponential improvement [6,8] only exists subject to an interesting but very strong conjecture.[1] Even worse, the Minkowsky bound is nonconstructive, and no methods are known which would allow one to construct a lattice which satisfies at least that bound in very high dimensions. Arguably the most important recent contribution in this respect has been given by Refs. [14,15] in which the problem is reduced, for any given dimension, to an infinite linear programming problem. The technique is powerful (in 8 and 24 dimensions the bounds are saturated by the best known packing, proving hence their global optimality) but has not yielded an understanding of the problem for generic d.

Given the complexity of the generic case it might prove useful to consider a simpler version of the problem. One of them is the so-called lattice packing problem, which restricts allowed packings to Bravais lattice packing only.[2] Although the set of possible packings is severely reduced, exact results

[1]For recent considerations of the applications of statistical mechanics to the Roger bound [9] see the work of Parisi [10]; see also Refs. [11–13].

[2]Two slightly different terminologies are being used in mathematics and physics with respect to lattices: mathematicians differentiate between lattices and periodic sets, while physicists talk about Bravais and non-Bravais lattices.

are established only up to $d \leqslant 8$, with the $d = 9$ case unlikely to be closed in the near future.

In theory the lattice sphere packing problem is simpler, because it admits an explicit algorithmic solution [16] where one has to check a finite number of special lattices to find the best one. The best packing, in fact, is both a perfect and eutactic lattice (we give the characterization of these lattices later), and both the number of perfect [16,17] and that of eutactic lattices are finite [18] (hence the intersection is). This algorithm has been applied to dimensions $d \leqslant 8$ to systematically find all such lattices [19–25]. In this paper we will run a randomized version of the algorithm in dimensions 8 to 19 to generate large (up to several millions) sets of perfect lattices in each dimension and then study the statistical properties thereof. We will introduce a fictitious temperature to explore nontypical regions of the space of perfect lattices and get the best known packings.

II. LATTICES, PERFECT LATTICES, AND EUTACTIC LATTICES

A. Notation

In this paper we will consider only lattices or in Physics terminology Bravais lattices, namely lattices which have only one particle per unit cell (see Fig. 1). A generalization of our results to an arbitrary but finite number of particles per unit cell will be discussed at the end of the paper. In our definitions and logic of discussion we will follow closely Schürmann [17], although we will not pretend to achieve the same level of rigor.

We will define a lattice A, one particle per unit cell, in $\mathbb{R}^d$ by means of the square matrix of the components of the d, d-dimensional linearly independent (basis) real vectors $\mathbf{e}^i$:

$$A = \begin{pmatrix} e_1^1 & e_2^1 & \dots & e_d^1 \\ e_1^2 & e_2^2 & \dots & e_d^1 \\ \vdots & \vdots & \ddots & \vdots \\ e_1^d & e_2^d & \dots & e_d^d \end{pmatrix}. \tag{1}$$

The points in the lattice are elements of the set

$$\Lambda = \{\mathbf{x} : \mathbf{x} = A\mathbf{z}, \quad \mathbf{z} \in \mathbb{Z}^d/\{\mathbf{0}\}\}. \tag{2}$$

The associated symmetric, positive definite d-by-d quadratic form Q is defined by matrix multiplication as

$$Q = A^T A. \tag{3}$$

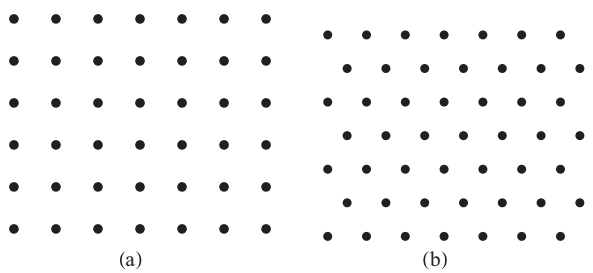

FIG. 1. (a) Square lattice. (b) Hexagonal lattice (also known as triangular lattice).

We will refer without a difference to the quadratic form Q or to the basis matrix A when we talk about a lattice. The distance of a point $A\mathbf{z}$ in the lattice is (here T stands for transpose, both of a vector and of a matrix)

$$l = ||\mathbf{x}|| = \sqrt{\mathbf{z}^T\, A^T A\, \mathbf{z}} = \sqrt{\mathbf{z}^T Q \mathbf{z}}, \tag{4}$$

where $\mathbf{z}^T Q \mathbf{z} = \sum_{i,j=1}^{d} z_i Q_{ij} z_j$.

The notion of *shortest vector* of a lattice is fundamental in the theory of lattices and allows one to connect to the theory of sphere packing. Namely, we define the *arithmetic minimum* of a lattice Q as the square of the minimum length of a vector in the lattice

$$\lambda(Q) = \min_{\mathbf{z} \in \mathbb{Z}^d/\{\mathbf{0}\}} \mathbf{z}^T Q \mathbf{z} \tag{5}$$

and the set

$$\mathrm{Min}(Q) = \{\mathbf{z} \in \mathbb{Z}^d : \mathbf{z}^T Q \mathbf{z} = \lambda(Q)\}. \tag{6}$$

Let us point out that the set $\mathrm{Min}(Q)$ should contain at least two vectors (as $\mathbf{x}$ and $-\mathbf{x}$ have the same length) but for the "interesting" lattices the cardinality of the set (known as the *kissing number*) is usually much larger, sometimes even exponential in d. The maximum cardinality of $\mathrm{Min}(Q)$ over the set of d-dimensional lattices is an open problem in most d and has been dubbed the *kissing number problem* [1].

The connection with the sphere packing problem is easily made. The largest nonoverlapping spheres we can fit in a lattice must have as radius half the length of the shortest vectors of Q. Considering that the volume of a unit cell is $\det A = \sqrt{\det Q}$, we have that the maximum fraction of space covered by a sphere packing Q is the ratio of the volume of this sphere divided by the volume of the unit cell:

$$\phi(Q) = B_d \frac{[\sqrt{\lambda(Q)}/2]^d}{\det(Q)^{1/2}}, \tag{7}$$

where B_d is the volume of a d-dimensional unit sphere:

$$B_d = \frac{2\pi^{d/2}}{d\,\Gamma(d/2)}. \tag{8}$$

A strictly related quantity is the Hermite constant of Q (in terms of which the packing fraction can be expressed):

$$H(Q) = \frac{\lambda(Q)}{\det^{1/d}(Q)}. \tag{9}$$

In the following we will also use another indicator that we will call "energy" as a target function to minimize with the introduction of a temperature:

$$e(Q) = -\frac{1}{d} \ln[\phi(Q)]. \tag{10}$$

The Minkowksy bound ensures that this quantity is bounded from below by the best lattices even in the limit $d \to \infty$.

The *lattice sphere packing problem* (henceforth LSP problem) in d dimensions is the problem of finding the maximum of $\phi(Q)$ [or $H(Q)$] among all the d-dimensional lattices. The problem is solved for $d = 1,\dots,8$ [19–25] and $d = 24$ [14,15] *only*.

B. Perfect lattices

We will now concentrate on a subset of lattices which turns out to be fundamental in the solution of the lattice sphere packing problem: the *perfect lattices*.

A lattice is named *perfect* iff the projectors built with its shortest vectors span the space of symmetric d-by-d matrices. So for a perfect lattice Q let Z be the cardinality of $\mathrm{Min}(Q)$ and let $\mathbf{v}_a \in \mathrm{Min}(Q), a = 1, \ldots, Z$ (Z is also called the *kissing number* of a lattice). Let M be any symmetric d-by-d matrix; there exists a set of real numbers μ_a such that

$$M = \sum_{a=1}^{Z} \mu_a \mathbf{v}_a \mathbf{v}_a^T. \tag{11}$$

For example, take the square lattice in $d = 2$:

$$Q_{\mathrm{sq}} = \begin{pmatrix} 1 & 0 \\ 0 & 1 \end{pmatrix}; \tag{12}$$

the shortest vectors are

$$\mathrm{Min}(Q_{\mathrm{sq}}) = \{(1,0),(0,1)\}, \tag{13}$$

and the projectors are

$$P_1 = \begin{pmatrix} 1 & 0 \\ 0 & 0 \end{pmatrix}, \quad P_2 = \begin{pmatrix} 0 & 0 \\ 0 & 1 \end{pmatrix}, \tag{14}$$

which do not span the space of symmetric matrices. Therefore the square lattice is *not* a perfect lattice.

Instead, consider the hexagonal lattice

$$Q_{\mathrm{hex}} = \begin{pmatrix} 2 & 1 \\ 1 & 2 \end{pmatrix}. \tag{15}$$

It has three shortest vectors (of length $\sqrt{2}$)[3]

$$\mathrm{Min}(Q_{\mathrm{hex}}) = \{(1,0),(0,1),(1,-1)\}, \tag{16}$$

and the corresponding projectors are

$$P_1 = \begin{pmatrix} 1 & 0 \\ 0 & 0 \end{pmatrix}, \quad P_2 = \begin{pmatrix} 0 & 0 \\ 0 & 1 \end{pmatrix}, \quad P_3 = \begin{pmatrix} 1 & -1 \\ -1 & 1 \end{pmatrix}, \tag{17}$$

and the reader can verify that they form a basis for symmetric 2-by-2 matrices (one can easily form linear combinations of the P to obtain the identity and two of the three Pauli matrices). Note that the number of shortest vectors of a perfect lattice is bounded from below by $(d+1)d$ since this is twice the smallest possible number of projectors that can span the space of symmetric matrices (the dimension of space of symmetric matrices). So in the previous example we could have said beforehand that the square lattice is not perfect, but we should have checked anyway that the hexagonal lattice was indeed perfect.[4]

Voronoi proved [16,17] that perfect forms are vertices of the Ryshkov polyhedron[5] defined as a set of forms Q whose shortest vector is larger than a given value:

$$\mathcal{P}_\lambda = \{Q : \lambda(Q) \geqslant \lambda\}, \tag{18}$$

where the actual value of λ (as far as $\lambda > 0$) is immaterial as the axes can be rescaled freely. Therefore we can reduce the sphere packing problem on $\mathcal{P}_\lambda$, hence constraining to forms with $\lambda(Q) = \lambda$ without any loss by finding

$$H = \frac{\lambda}{\inf_{Q \in \mathcal{P}_\lambda} \det^{1/d}(Q)}. \tag{19}$$

The number of vertices of the Ryshkov polyhedron and hence of perfect forms is (up to isometries that we define below) finite (a small subset of all the lattices in any given dimension d).

The main result which gives importance to perfect lattices in the context of the LSP problem is the classic *Voronoi theorem*, which can be stated as follows:

Theorem: The best lattice sphere packing is a perfect lattice.

The proof (which we do not give here; see Ref. [17]) follows if one shows that $\det^{1/d}(Q)$ *does not have stationary points inside the Ryshkov polyhedron*. This in fact implies that the minimum of $\det(Q)$ and the maximum of ϕ (or H) occur on the vertices of the polyhedron, hence on perfect lattices.

Therefore the problem of LSP is reduced to finding all the perfect lattices and comparing their packing fractions: It becomes a problem for a computer to solve.[6] Unfortunately (or maybe, fortunately) things are not so easy as they might seem. Indeed, the number of perfect lattices grows very fast with the dimension (probably faster than exponential, as we will argue later) and the task of finding them all has been completed up to $d = 8$ (where they are 10 916). For $d = 9$ one has found 5×10^5 forms [26], but the conjectured total number should be about 2×10^6.

C. Isometry of lattices

A lattice admits many equivalent representations in terms of quadratic forms Q: One can rotate the lattice or replace its basis vectors with their independent linear combinations. This equivalence is captured by notion of *isometry*:

Definition: Lattices Q and Q' are isometric if there exists a matrix $U \in \mathrm{GL}_d(\mathbb{Z})$ and $c \in \mathbb{R}$ such that

$$Q' = c\, U^t\, Q\, U.$$

Another name in use is *arithmetical equivalence*. For example, the hexagonal lattice Q_{hex} given by Eq. (15) has

[3] We remind the reader that the length of a vector is $(\mathbf{x}^T Q \mathbf{x})^{1/2}$.

[4] In $d = 2$ it turns out that 6 (3 shortest vectors and their opposite $-\mathbf{x}$) is also the maximum *kissing number* achievable among lattices (and among general point patterns too).

[5] The Ryshkov polyhedron is not a finite polyhedron but is a *locally finite* polyhedron. This difference turns out to be immaterial here.

[6] In principle LSP is an algorithmically solvable problem even without restricting to perfect lattices, since the number of Bravais lattices is finite in any dimension (for example, there are 14 such lattices in three dimensions, 64 in four dimensions, and the number should rapidly increase with d). However, the mere enumeration of Bravais lattices is an unaccomplished task in $d \geqslant 7$, and to our knowledge no algorithm for generating them sequentially exists. Restricting the problem to perfect lattices simplifies it considerably.

an equivalent representation

$$Q'_{\rm hex} = \begin{pmatrix} 2 & -1 \\ -1 & 2 \end{pmatrix},$$

which is isometric to $Q_{\rm hex}$ with isometry matrix

$$U = \begin{pmatrix} 1 & -1 \\ -1 & 0 \end{pmatrix}.$$

A practical way of checking if a given pair of forms are isometric was developed in Ref. [27] where one uses backtrack search to construct an isometry matrix (if this exists). However, most of the times it is sufficient to check if some criteria (like the number of shortest vectors) are satisfied before running the generic code, which can be quite slow in high dimensions.

D. Eutaxy

The last concept that we need for our investigation is that of *eutactic* lattice. This is not strictly necessary for understanding our results in this paper, but it gives a suggestive connection with the theory of spin glasses, which we plan to investigate as a continuation of this work. Eutactic lattices cannot be improved (as we will prove below) by an infinitesimal transformation of the matrix base and therefore are local maxima of the packing fraction. Their number also grows with the dimension d, and one is then led to think that in high enough dimensions this phenomenon is reminiscent of the landscape of a mean-field spin glass free energy [28].

Given a perfect form Q we can always write (since it is a symmetric, nonsingular matrix) its inverse Q^{-1} in terms of the projectors built on its shortest vectors

$$Q^{-1} = \sum_{x \in {\rm Min}(Q)} \alpha_x \, \mathbf{x}\mathbf{x}^T \tag{20}$$

(here $\mathbf{x}\mathbf{x}^T$ is the matrix with elements $x_i x_j$).

Definition: Eutactic form is one for which one can choose all the above $\alpha_x > 0$. An equivalent definition is that Q^{-1} is in the interior of the Voronoi domain of the perfect form Q, defined as

$$\mathcal{V}(Q) = {\rm cone}\{\mathbf{x}\mathbf{x}^T : \mathbf{x} \in {\rm Min}(Q)\}, \tag{21}$$

the cone in the space of forms generated by the projectors built with the shortest vectors of Q.

The Hermite constant (or packing fraction) of an eutactic form can be decreased by any infinitesimal change of the form. In fact, by using the identity

$${\rm Tr}\,[(\nabla \det Q)A] = \det(Q){\rm Tr}\, Q^{-1}A, \tag{22}$$

we obtain, to first order in $\delta Q = Q' - Q$ where $Q' \in \mathcal{P}_{\lambda(Q)}$ (so the length of the minimal vectors is unchanged)

$$H(Q + \delta Q) = H(Q) - \frac{\lambda/d}{\det^{1/d}(Q)} {\rm Tr}(Q^{-1}\delta Q) < H(Q), \tag{23}$$

where the inequality follows from

$${\rm Tr}(Q^{-1}, Q' - Q) = \sum_{\mathbf{x} \in {\rm Min}(Q)} \alpha_{\mathbf{x}} (\mathbf{x}^T Q' \mathbf{x} - \mathbf{x}^T Q \mathbf{x}) > 0, \tag{24}$$

as $Q' \in \mathcal{P}_{\lambda(Q)}$ and $\alpha_{\mathbf{x}} > 0$.

It follows then that *a perfect and eutactic lattice is a local maximum of H* from which we obtain the following theorem:

Theorem: Perfect and eutactic (PE) lattices are local maxima of the Hermite constant and hence of the packing fraction

and therefore

Corollary: The best packing lattice is both perfect and eutactic.

The concept of eutaxy is extended to arbitrary lattices with introduction of *weakly eutactic*, *semi-eutactic*, and *strongly eutactic* lattices. Weakly eutactic lattices satisfy Eq. (20) with real coefficients α_x, semieutactic lattices have $\alpha_x \geqslant 0$ [i.e., some of the coefficients in Eq. (20) are zero], and finally strongly eutactic lattices are eutactic lattices with all α_x equal. Recall that by definition a perfect lattice is (at least) weakly eutactic since $\mathbf{x}\mathbf{x}^T$ span the space. The interest in strongly eutactic lattices comes from the fact they are also the best packers locally among lattices with arbitrary number of particles per unit cell [29].

The problem of determining eutaxy class of a form admits an efficient solution: Given a form, its eutaxy class, either non-eutactic, weakly eutactic, semi-eutactic, or strongly eutactic, can be decided by solving a sequence of linear programs [25] and therefore is of polynomial complexity with respect to the number of shortest vectors (which, however, can grow as fast as an exponential of d).

Summarizing, the take-home messages of this section are that the maximum of the packing fraction over lattices in any given dimension is attained by one of the PE lattices, of which there is a finite number (in any given d) and that each of the PE lattices is a local maximum. This characterization is extremely powerful but still does not prevent us from having to find all perfect lattices and checking which ones are eutactic and which are not. There is a simple and efficient way to generate perfect lattices, but there is not (as far as we know) a similarly efficient way to generate eutactic [30,31] or PE lattices. One should first generate perfect lattices and then check them for eutaxy. The simple and efficient way to generate perfect lattices is given by the Voronoi algorithm, which we review in the following section.

III. THE VORONOI ALGORITHM AND ITS RANDOMIZATION

We have now reduced the problem of finding the best lattice packing to that of finding the best lattice packing among perfect and eutactic lattices. We need a way to generate all the perfect lattices, select the eutactic ones, and look at the most dense among them. The first task is accomplished by the *Voronoi algorithm* [16,17,32], which we now describe.

Start with a perfect form Q.

(1) Find all the shortest vectors $\mathbf{x} \in {\rm Min}(Q)$, and the inequalities describing the cone $\mathcal{V}(Q)$:

$$\mathcal{V}(Q) = \{Q' | \, \forall \mathbf{x} \in {\rm Min}(Q) : \mathbf{x}^T Q' \mathbf{x} \geqslant 0\}. \tag{25}$$

(2) Find all the extreme rays of the polyhedral cone $\mathcal{V}(Q)$. Call them $R_1, \ldots, R_k$.

(3) Create the forms $Q_i = Q + \alpha_i R_i$, choosing rational numbers α_i such that the new form Q_i is again perfect.

(4) Check for isometries and repeat from Start with each of the genuinely new Q_i.

In this way we are guaranteed to find all the perfect forms. If we check for isometry with previously found forms the algorithm will at a certain point terminate, its output being the list of all perfect forms in a given dimension. The extreme rays of an n-dimensional polyhedral cone are the half-lines at which at least $n-1$ inequalities are binding [$n = d(d+1)/2$ here]. The bottleneck of the algorithm is finding all the extreme rays R_i of a given lattice Q [33] [or more rigorously of the Voronoi domain $\mathcal{V}(Q)$], which, since the number of minimal vectors can be quite large (as much as exponential in d), can be a complicated linear programming problem. The generic version of this problem is known as a *polyhedral representation conversion* problem in polyhedral geometry computation community, and its complexity is currently unknown [33,34]. All the forms generated from a given form Q are called *neighbors of* Q, and the graph consisting of perfect forms linked to their neighbors is called the *Voronoi graph* of perfect forms in a given dimension d. Importantly, the graph is connected and starting from any vertex one can at least in principle reach any other vertex of the graph [16,17,32].

Thus generated lattices might (and often do) have generating forms with rather large norms of basis vectors. For example, we know there is just a single perfect form in $d = 2$. A plain random walk would generate forms with entries growing as a function of the step number. To remedy this problem we use the fact that for a given lattice its basis can be transformed to an equivalent basis but with reduced basis vector norms. Figure 2 illustrates this idea for a square lattice. The exact transformation which reduces the norms to the smallest possible value is expensive, and we use a inexact one known as the LLL reduction after the names of the authors [35] to produce equivalent representations of lattices with rather short basis vectors. Technically we apply the LLL reduction on every newly generated form: This extra step allows us to generate forms with relatively small entries. Coming back to $d = 2$ case we find just three distinct forms (all of which are isometric). It is worth pointing out that the probability of generating isometric forms becomes much less relevant for higher dimensions and completely irrelevant for $d \geqslant 13$. The LLL reduction is also a subset of isometry testing and actually removes the most trivial isometries. In order to focus on higher dimensions we propose to *randomize* the Voronoi algorithm, namely, to introduce a randomized subroutine to find an extreme ray R_i. In this way we do not have to find all the extreme rays but just pick one and move in that direction.

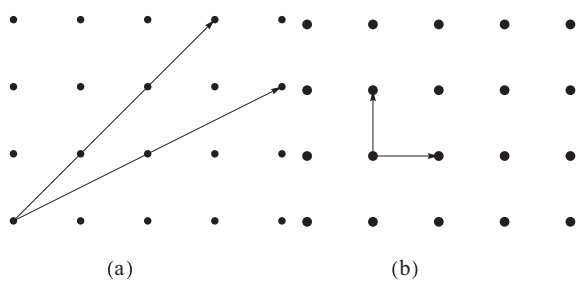

FIG. 2. Example of lattice reduction for a square lattice: random initial basis (a) where basis vectors have large norms. After lattice reduction (b) one gets "short" basis vectors.

We do the following: We slice the cone $\mathcal{V}(Q)$ with a plane; in this way the extreme rays become vertices of a polytope. We then define a random linear cost function

$$f(Q') = \sum_{i,j=1}^{d} A_{ij} Q'_{ij}, \tag{26}$$

where the A_{ij} are Gaussian random variables, and we solve the corresponding linear programming problem $\max_{Q' \in \mathcal{V}(Q)} f(Q')$. Linear functions are necessarily maximized at the vertices of the polytope, and therefore in this way we select randomly an extreme ray, which gives a neighbor of Q. The Gaussian distribution of the A_{ij} induces a distribution on the frequency each neighbor is visited with which is far from uniform (a vertex is visited more often if in the polyhedron it is surrounded by facets with relatively large surface). We will discuss later our attempts to make more uniform this distribution.

We have now defined the random generation of a new neighbor of Q, so in order to define a random walk we need to define the rules for accepting or rejecting said moves.

IV. MONTE CARLO PROCEDURE AND THE VORONOI GRAPH

It is clear that if we are only interested in the structure of the Voronoi graph we should run a random walk as unbiased as we can. Of course, the most naturally unbiased algorithm would ideally generate any neighbor with equal probability. However, this would be equivalent to finding all the neighbors for every perfect lattice; this problem can be incredibly difficult, and it has been solved only for $d \leqslant 8$ [24], with a large use of computer resources, so we do not attempt to solve it here.

A. A warm-up: Simple cases $d \leqslant 7$

As a warm-up we study very low dimensions: For $d \leqslant 7$ the problem of enumeration of perfect lattices is relatively simple due to small number of nonisometric perfect forms $\mathcal{N}$:

Dimension	1	2	3	4	5	6	7
$\mathcal{N}$	1	1	1	2	3	7	33

The problem is completely trivial for $d \leqslant 3$ since there is a single perfect lattice (up to isometries). For $d = 4,5$ enumeration is trivial: Our code finds the other forms on the first steps. Less trivial cases are $d = 6$ and $d = 7$ with 7 and 33 perfect forms, respectively (the Voronoi graphs are shown in Fig. 3). It takes about 1000 steps to find all 7 forms in $d = 6$. In $d = 7$ we recover 32 forms after 10^6 steps.

B. Properties of the $d = 8$ and $d = 9$ Voronoi graphs

We compare the random walk on the exact Voronoi graph as found in Ref. [24] with the numerical results of the previously described randomized Voronoi algorithm.

The Voronoi graph for $d = 8$ is quite an interesting object if seen through the lens of statistical mechanics of random

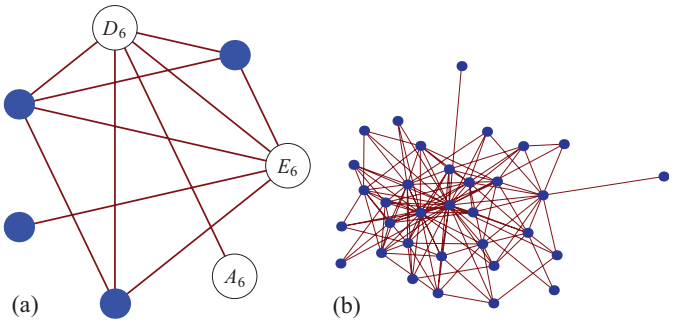

FIG. 3. (Color online) (a) The Voronoi graph in $d = 6$; vertex 1 is E_6, vertex 3 is D_6, vertex 7 is A_6. (b) The Voronoi graph in $d = 7$; there are just 33 perfect forms. The central point is E_7; it is connected to all the other vertices but A_7, which is the rightmost vertex of the graph.

graphs. We unveil here only a small set of observations. The number of vertices is the number of perfect forms, namely, 10 916, and we put an edge whenever two forms are the Voronoi neighbors. The most connected form is the densest packing E_8, which has 10 913 neighbors, and it is interesting to notice that the distribution of the connectivity of the graph follows quite closely a power law decay (a so-called *scale-free* network) for $c \lesssim 150$ as we see in Fig. 4. Over this two orders of magnitude range we can fit the connectivity distribution by the law

$$p(c) \propto c^{-(2.5\pm0.1)}, \tag{27}$$

which defines a critical exponent. We will see that this is also the case in $d = 9$.

It follows from the large connectivity of E_8 that an unbiased random walk on this graph would visit E_8 a large number of times. By running a completely unbiased random walk on the *exact* Voronoi graph in eight dimensions we find that E_8 should be visited about 1.6% of the times (this has to be compared with an average of $1/10\,916 \simeq 0.01\%$). In our algorithm we see, however, that this number is much larger: E_8 is visited about 80% of the time. This means that our algorithm is biased towards lattices with higher connectivity even more than an unbiased random walk is. This has to do with the large surface occupied by facets of the Ryshkov polyhedron enclosed by rays generating E_8.

This is a common feature in any dimension: The densest lattices are reached quite fast by our randomized algorithm even in the absence of any *a priori* bias towards them. The balance between the increase in the attractivity of the best packers and the increase in the size of the graph allows one to stumble upon the densest lattice up to $d = 12$ with a few hundred trials without having to bias the random walk towards the densest lattices. Moreover, as a typical scale-free network, the diameter of the Voronoi graphs will be quite small, scaling as the logarithm of the number of vertices divided by average of the logarithm of the connectivity.

We now discuss the results of our randomized algorithm in $d = 8$. We find, as said, that 80% of the times is spent on E_8. The remaining 20% of the time is divided among the remaining lattices. Every time a lattice is visited, an isometry test is run against the previously visited lattices. If it is new, it is added to the list; in any case a link between the two

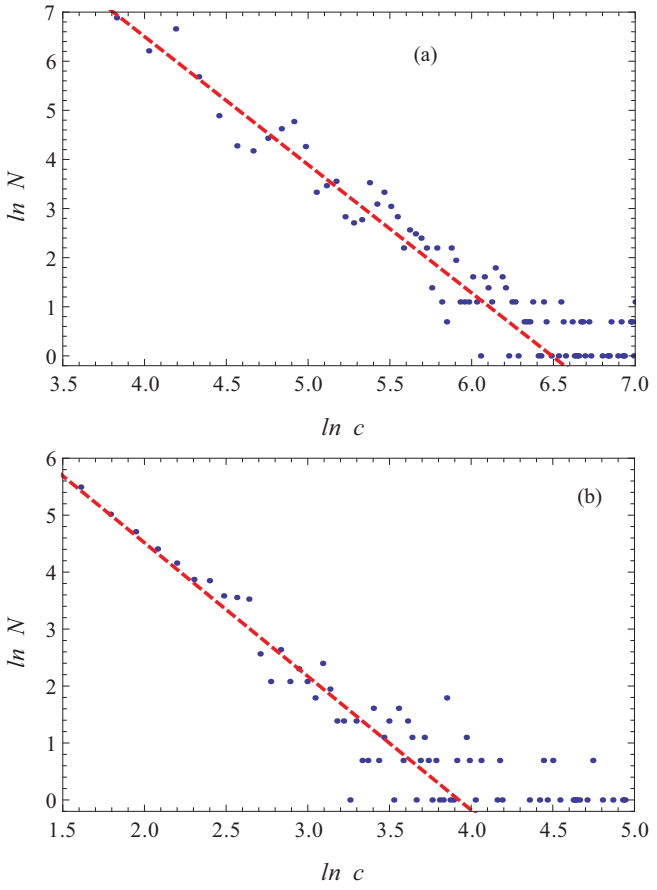

FIG. 4. (Color online) (a) The distribution of the connectivity of the $d = 8$ Voronoi graph, exact results. (b) The same distribution sampled with the randomized Voronoi algorithm. N is the number of perfect lattices with connectivities between c and $c + \delta c$, where $\delta c = 10, 1$ for the exact and sampled cases. The power-law fit is described in Eq. (27). In general, an underestimation by the random walk of the connectivity of the nodes is observed, but a power law fit still works well, and the power law is compatible with the exact result (see text).

lattices is added to the list of edges in the graph. In this way, in 10^6 runs we generate about 3×10^3 nonisometric perfect lattices (out of 10 916). This might be taken as a measure of the importance of isometry as well as of the dominance of E_8 in eight dimensions.

In $d = 9$ we run the randomized Voronoi algorithm for 5×10^6 steps, and we generate about 3×10^5 nonisometric perfect forms. We recall that in $d = 9$ the Voronoi graph is conjectured to be made of about 2×10^6 inequivalent perfect forms. We hence find in this case that the importance of isometry is much reduced. We will see that in higher dimensions the isometry test becomes irrelevant as randomly generated forms turn out to be almost always nonisometric.

By looking at the distribution of the local connectivity in Fig. 5(a) we see that also in this case a power-law distribution is the best fit over three orders of magnitude:

$$p(c) \propto c^{-2.5\pm0.1}. \tag{28}$$

We also observe the same slight overestimate of the fraction of low-connectivity graphs we saw in $d = 8$. This is due (as in

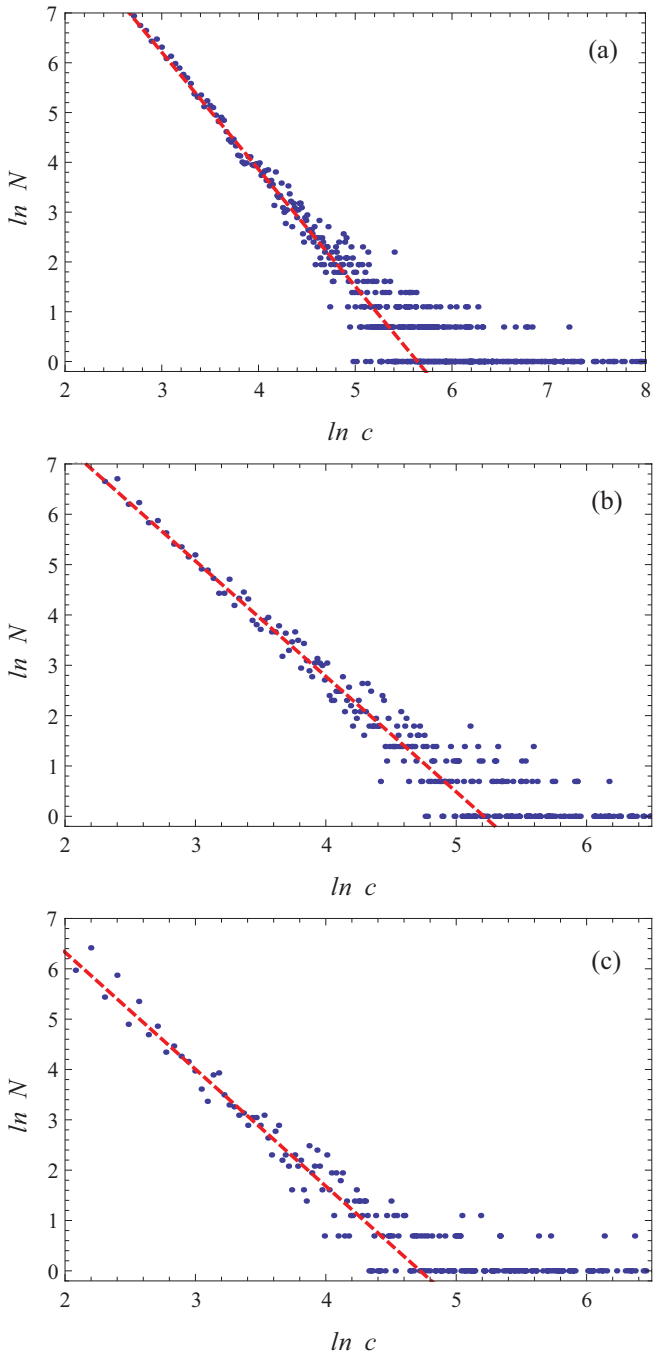

FIG. 5. (Color online) The distribution of the connectivity of the $d = 9$ (a), $d = 10$ (b), and $d = 11$ (c) Voronoi graphs estimated by the random walk. $N(c)$ is the number of perfect lattices with connectivity c. The power-law fit is described in Eq. (28).

other dimensions) to the fact that in order to assign a connectivity c to a graph the random walk has to visit said graph at least c times. There is no proved estimate of the number of perfect lattices (size of the Voronoi graph) as a function of dimension. The sequence looks like $1,1,1,3,7,33,10\,916, \sim 2 \times 10^6, \ldots$ and suggests a superexponential growth, for example, like $e^{A\,d^2}$. Consequently the number of steps required for an accurate estimation of connectivity grows rapidly. This means

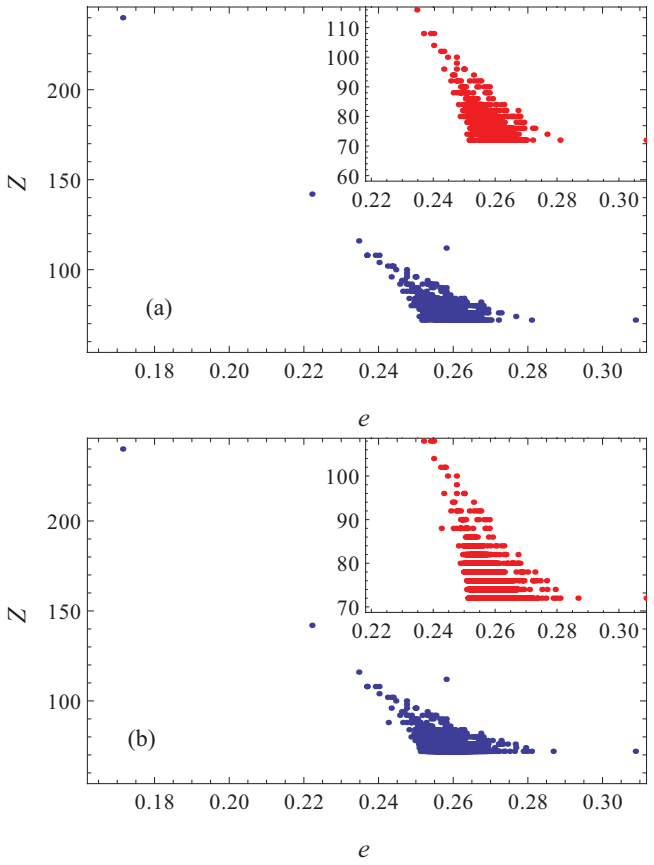

FIG. 6. (Color online) (a) Kissing number vs energy ($d = 8$), generated set. (b) Kissing number vs energy ($d = 8$), exact data. The insets show same plots with kissing numbers $Z \leqslant 110$. In both cases the best packer and kisser is alone in the upper left of the figures.

that for dimensions higher than nine a different strategy has to be used.

However, after observing the similarity between the two exponents for the connectivity distribution and checking our random walk results against the exact results in $d = 8$, it is nothing but tempting to *conjecture* that the *Voronoi graph is a scale-free random network in any dimension* and that *the exponent of the distribution of the connectivity is about* 2.4–2.5. With the above proviso we also checked $d = 10,11$ and found $p(c) \sim c^{-2.4}$ as shown in Fig. 5(b) and 5(c).

One can also plot (see Figs. 6 and 7) the joint distribution of kissing number and energy observing how the best packers have largest kissing number, and they are both rare events with respect to the typical distribution. This phenomenon is constant across all dimensions.

V. BIASING THE RANDOM WALK WITH A TEMPERATURE

Following a common trick in statistical mechanics we introduce a temperature β as a Lagrange multiplier for the packing fraction. We therefore would like to define a statistical

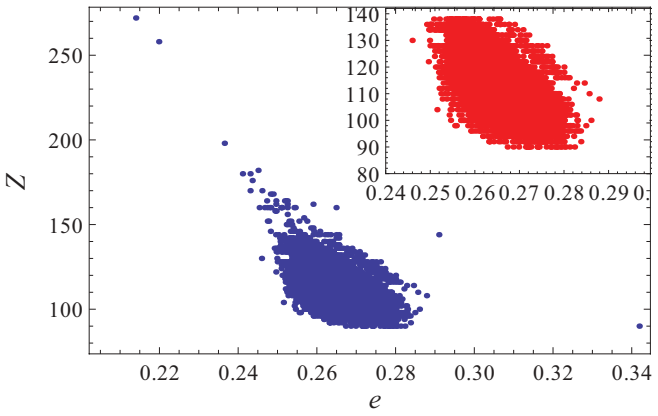

FIG. 7. (Color online) Kissing number vs energy ($d = 9$). The inset shows detailed plot for kissing numbers $Z \leqslant 140$.

ensemble described by the partition function:

$$Z = \sum_{Q} \mu(Q)\, e^{-\beta\, d^2\, e(Q)},$$
$$e(Q) = -\frac{1}{d} \ln \phi(Q), \tag{29}$$

where Q is a perfect lattice in d dimensions and $\mu(Q)$ is the measure induced on the space of perfect lattices by the solution of the linear program (26);[7] namely, $\mu(Q)$ is the fraction of times the lattice Q is visited when the random walk described in the previous section is run. We also defined *energy of a packing* $e(Q)$ thus in (10) that it is a quantity of order 1 for the best packings which have a packing fraction decreasing exponentially in dimension. Quite conveniently the best packings translate into packings with lowest energy, i.e., "ground states." The normalization for the temperature is due to the expectation that for the densest lattices $\ln(\phi) \sim d$ (as both upper and lower bounds predict), and we need the exponent to be the order of the number of degrees of freedom, namely, $\sim d^2$.

By lowering the temperature we expect to explore the regions of the Voronoi graph in which lattices are denser.

VI. RESULTS

Below we present the numerical results generated by random walks described above and their interpretation.

A. Aims

The generation procedure is inherently stochastic, and we do not aim at generating complete sets of perfect lattices in a given dimension. As we already mentioned we have discovered 32 and approximately 3×10^3 forms after 1000 and $\sim 10^6$ runs in $d = 7$ and 8, respectively. The number of discovered forms in $d = 8$ increases with extra runs, although a complete enumeration would require a huge number of runs.

Such a huge number of perfect lattices suggests a statistical approach so that properties of typical or even dense lattices can be extracted from a subset of the complete set. Thus our goal is rather to generate sufficiently large, representative sets of perfect forms in a given dimension which would allow us to understand typical properties of perfect lattices and spot any universal pattern behind.

The fact that we are dealing with relatively large sets of forms together with the stochastic nature of the generating procedure allows to introduce empirical distributions of various characteristics of lattices. We are going to focus mainly on two quantities: *energy*, which was defined above, and *kissing number*. Both quantities are of interest with respect to the best packings. We will analyze their statistical properties, in particular, their distributions and moments on the ensemble generated by the random walk.

We have generated random walks (both simple and biased) in dimensions from 8 to 19. Complexity of computation gradually increases with dimension as does typical running time to generate sufficiently representative set of lattices. Running times vary from about an hour in $d = 8,9$ to 5–7 days in $d = 19$ to generate 5×10^4 lattices. Higher dimensions, i.e., $d \geqslant 20$ are accessible, the difficulties encountered being rather of a technical than a conceptual nature.

B. Random walk at infinite temperature

We have first performed runs in different dimensions at infinite temperature which correspond to plain random walks: Departing from an initial lattice one computes a random neighbor and hops there. It is natural to think that in this way one generates typical perfect lattices.[8] The walk terminates after a finite number of steps N have been made. The averages $\langle \dots \rangle$ are simple summations normalized by N.

Typically A_d was used as a starting point of a random walk for $d \leqslant 12$ and D_d was used for $d \lesssim 16$ since here the energy of A_d becomes too high. In even higher dimensions ($d > 16$) the energy of D_d itself becomes too high for D_d to be a good starting point, and we used different initial lattices with better packing fractions which we generated by chain runs, that is, first running a random walk starting at D_d and then picking a suitably dense lattice as a starting point for a new random walk.

As already mentioned our randomized code is biased towards denser lattices, and it does not sample all lattices uniformly like a complete enumeration would do (this effect is *on top* of the bias given by the larger connectivity of the densest lattices). It is instructive to compare our results to exact data. Unfortunately the latter are known only for $d < 9$,[9] and there are too few perfect lattices for our approach to be beneficial for $d < 8$. So we start by comparing energy and kissing number

[7] In practice we introduce the temperature on the random walk via Monte Carlo sampling, but since we cannot ensure that the detailed balance holds for our randomized Voronoi algorithm, we cannot ensure that we are quantitatively sampling the partition function above. For the purpose of this paper this is a minor point.

[8] Remember that there is already a bias built in into generation of neighbors.

[9] Enumeration in $d = 9$ is in progress; see Ref. [26]. Partial results are available, but due to nature of the enumeration procedure they are biased and cannot be directly compared to our data.

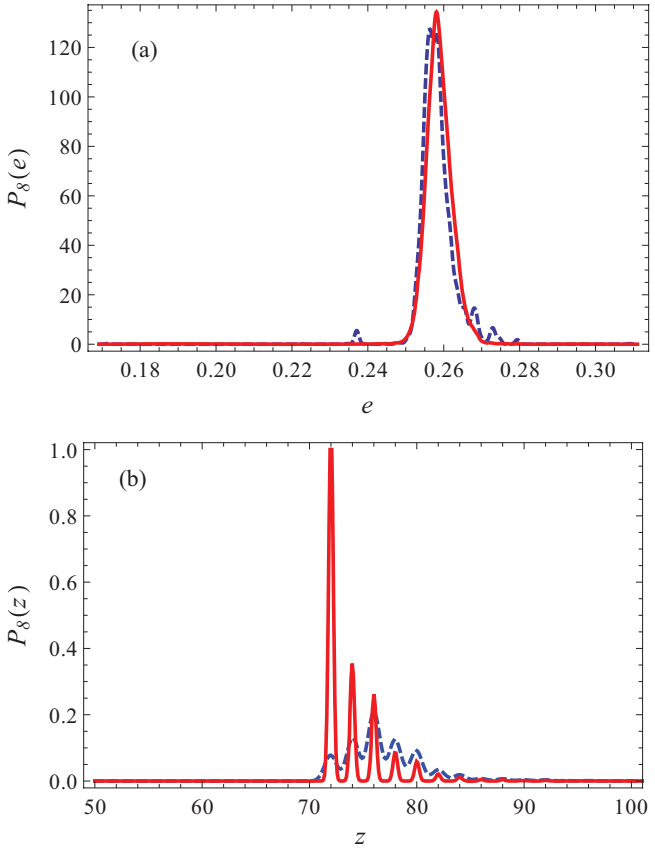

FIG. 8. (Color online) Comparison of exact and empirical distributions generated by the randomized Voronoi algorithm. (a) Distribution of energies e from the randomized Voronoi algorithm with isometry testing (blue/dashed) and exact distribution (red/solid) for $d = 8$. (b) Same comparison of distributions of kissing numbers from the randomized Voronoi algorithm with isometry testing (blue) and exact distribution (red) for $d = 8$.

distributions as sampled by our code and their exact values in $d = 8$ shown in Fig. 8. We see a reasonable agreement between the exact data and the ones generated by the randomized algorithm. This allows us to assume that data generated by the randomized Voronoi algorithm are representative and unbiased, and we use data generated in higher dimensions where no exact data are available. The discrepancies present can be attributed to fluctuations associated to stochastic nature of our algorithm. This is especially clear for the kissing number which is integer by definition.

A rough measure of representativity of a sample generated by a random walk is whether it visits "dense" lattices with high kissing numbers, or even better, the densest (known) lattice in that dimension. For low dimensions, $d < 13$, just $N_d = 10^4$ runs were enough to satisfy this requirement. Starting with $d = 13$ one has to make more runs (although in $d = 13$ a random walk of 10^4 steps comes quite close to the best packing: $e = 0.28$ and $e_{\text{best}} = 0.27$). The required number of steps N_d is growing fast: $N_{13} \sim 10^5$, while $N_{14} > 10^5$. The situation quickly deteriorates in higher dimensions: While in $d = 8$ the random walk is hitting E_8 about 80% of the time, the number drops down to $< 1\%$ of hits for Λ_{10} (the best known lattice packing in $d = 10$) and goes further down for higher d. Table I

TABLE I. Frequencies with which a best known packing is visited by a random walk as a function of dimension.

Dimension	8	9	10	11	12
Frequency	0.835	0.341	0.096	0.0156	0.00191

gives frequencies for a random walk to visit the best packers in $d = 8 - 12$. The data seem to suggest a faster than exponential decay, a simple fit giving $\sim e^{-7.0\, x^{1.92}}$.

Table II gives a summary on average energies, their standard deviations σ_e, best found, worst found, and best known lattice for $d = 8$–19 (N is number of steps in random walk): The standard deviation clearly decreases with dimensions; the increase for $d = 17$–19 indicates that more runs are required to get a representative set of lattices. Indeed, comparing the behavior of the deviation with number of runs for $d = 17$ (See Table III), one sees the decrease as the number of runs increases (the same behavior is present in $d = 18, 19$): The decrease of standard deviation suggests that distribution of energies $\mathcal{P}_d(e)$ is concentrating around the mean value and becomes peaked around its mean value for large d:

$$\mathcal{P}_{d\to\infty}(e) \sim \delta(e - \langle e\rangle_{d\to\infty}). \tag{30}$$

Figure 10 shows behavior of average energy (no checks for isometry) with dimension. Large deviations in low dimensions up to $d < 12$, represented by error bars on the figure, are related to the fact that the distribution of energies in these dimensions is highly irregular if no check for isometry is performed during the random walk (see Fig. 9, case of $d = 8$ for an illustration).

An important issue is equivalence or isometry of generated lattices. As we have discussed above a single lattice admits many equivalent representations in terms of quadratic forms. One might worry if random walk is generating many or few equivalent lattices. The above results were generated neglecting isometry partially: Only the LLL reduction was performed on newly generated forms. Based on $d = 7, 8$ results we know that isometry is definitely important in low dimensions. However, it is relevant only for low dimensions,

TABLE II. Average energies of perfect lattices for $d = 8, \ldots, 19$. Sample sizes N are 10^6 for $d = 8$–12, 10^5 for $d = 13$–16, 2×10^5 for $d = 17, 18$, and 1.5×10^5 for $d = 19$. The observed increase of standard deviation σ_e for $d > 17$ indicates that sample size was not big enough. Increasing the sample size decreases the deviation.

Dim.	$\langle e\rangle$	σ_e	Best found	Worst found	Best known
8	0.180572	0.021502	0.171465	0.308792	0.171465
9	0.23352	0.01823	0.21396	0.34188	0.21396
10	0.26828	0.01422	0.23857	0.37285	0.23857
11	0.29347	0.01228	0.25511	0.40193	0.25511
12	0.31505	0.00796	0.25055	0.38024	0.25041
13	0.33106	0.00328	0.27179	0.40709	0.27178
14	0.34277	0.00236	0.31862	0.43265	0.27386
15	0.35405	0.00273	0.33522	0.45703	0.27218
16	0.36507	0.00197	0.34235	0.48031	0.26370
17	0.37205	0.00280	0.33949	0.50258	0.27833
18	0.38322	0.00235	0.37805	0.39238	0.28489
19	0.39000	0.00391	0.37909	0.40146	0.28903

TABLE III. Standard deviation of energy in $d = 17$ as a function of number of runs N.

N	10^4	10^5	2×10^5
Deviation	0.0064997	0.0030565	0.0028058

our data suggest $d < 13$, where the number of perfect lattices is relatively small and random walks of moderate size contain many isometric copies of the same lattice. For higher dimensions, $d \geqslant 13$, where the number of perfect lattices is huge, the chance of hitting an isometric lattice is vanishingly small except for the densest lattices, which have a larger isometry family. This is illustrated by Fig. 9, which compares probability distributions of energies for $d = 8$ and 12. It is worth stressing that this statement holds true only if one samples a relatively small subset of all perfect lattices. Once sample size is comparable to the size of the full set of perfect forms, isometry becomes important in any dimension. This fact can in principle be used to define a formal criterion whether one has generated a representative sample. Including isometry test in generation procedure is easy: Every newly generated form is checked for isometry against all previously generated forms.[10]

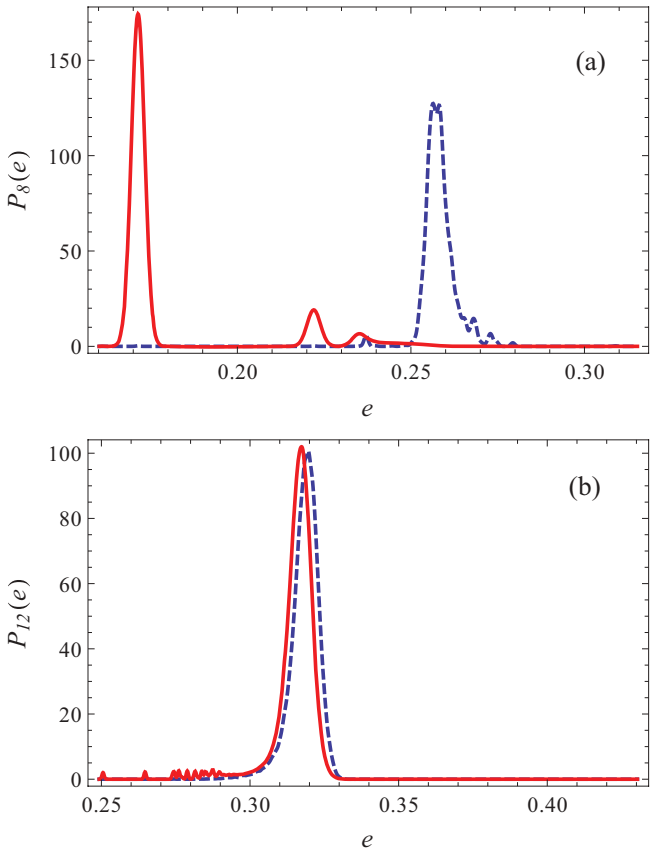

FIG. 9. (Color online) (a) Distribution of energies e with isometry test (blue/dashed) and without (red/solid) the test in $d = 8$. Isometry is very important and the two distributions are completely different: Without isometry check distribution concentrates around the energy of E_8. (b) Distribution of energies e with (blue/dashed) and without (red/solid) isometry test in $d = 12$. Isometry is no longer important, and the distributions are almost the same, except the low energy tail, where one still sees small spikes.

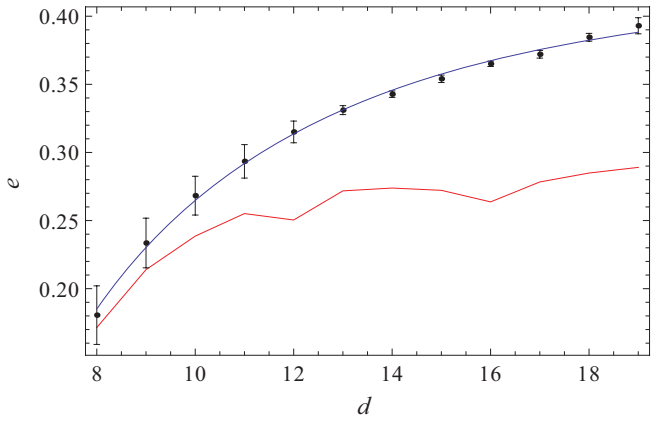

FIG. 10. (Color online) Average energy $\langle e \rangle = -\frac{1}{d}\langle \ln \varphi \rangle$ of a random walk as a function of dimension ($d = 8 - 19$) (black dots). Error bars correspond to standard deviation of energy. The smooth curve (blue/top) is a guide to the eye. The red curve (bottom) is the energy of the best known lattice packings.

The effect of isometry on energy average $\langle e \rangle$ is to increase values for low dimensions, which are dominated by dense lattices if no isometry checks are performed. The higher-dimensional data, $d > 12$, are left intact since isometry becomes completely irrelevant. We reproduce in Table IV the $\langle e \rangle$ curves for data with isometry checks. We see the same trend of decreasing standard deviation with increase of dimension as in the case of no isometry testing.

In what follows we use a mixed set of data: Samples with isometry checks for $d < 13$ and samples with no isometry testing applied for $d > 11$. We do so to remove features specific to low dimensions $d < 13$ and reveal the generic features common with dimensions $d > 11$.

Let us concentrate on two possible scenarios, the simplest cases where to locate our typical lattices. On one hand we can for example look at the energies of A_d, D_d families of lattices [7]:

$$e(A_d) = \frac{1}{2}\ln\frac{2}{\pi} + \frac{\ln(1+d)}{2d} + \frac{1}{d}\ln\Gamma\left(1+\frac{d}{2}\right) \tag{31}$$

$$\simeq \ln(d)/2 + O(1), \tag{32}$$

$$e(D_d) = -\frac{1}{2}\ln\pi + \left(\frac{1}{2}+\frac{1}{d}\right)\ln 2 + \frac{1}{d}\ln\Gamma\left(1+\frac{d}{2}\right)$$

$$\simeq \ln(d)/2 + O(1). \tag{33}$$

Both A_d and D_d have asymptotically equal energies for $d \to \infty$: $\sim \ln d/2$, which means the subexponential packing fraction.

The Minkosky and the Kabatiansky-Levenstein bounds tell us that there are lattices with only exponentially small packing fraction. Asymptotically in large dimensions, upper and lower

[10] See Appendix B for more details.

TABLE IV. Comparison of energy averages $\langle e\rangle$ without and with isometry test. Additionally exact values of average and standard deviation are given for $d = 8$.

d	$\langle e\rangle$	Std(e)	$\langle e\rangle_i$	Std$_i(e)$	$\langle e\rangle_{\rm ex}$	Std$_{\rm ex}(e)$
8	0.180571	0.021502	0.258296	0.0050364	0.258845	0.003593
9	0.233521	0.018231	0.266341	0.005073	0.259662[a]	0.006006[a]
10	0.268281	0.014227	0.281615	0.005484	–	–
11	0.293471	0.012288	0.299142	0.005262	–	–
12	0.31506	0.007967	–	–	–	–

[a]Values for $d = 9$ are extracted from partial enumeration [26].

bounds give

$$e_M = \ln(2) + O[\ln(d)/d], \tag{34}$$

$$e_{\rm KL} = 0.413\ldots, \tag{35}$$

and it is worth remembering the Torquato-Stillinger conjectured bound which should replace Minkoswky's under an appropriate hypothesis on high-dimensional lattices [6,8]:

$$e_{\rm TS} = 0.539 + O[\ln(d)/d]. \tag{36}$$

Random walks in high dimensions are sampling lattices with energy close to its mean value $\langle e\rangle$. We try two fits for this function of d, one with the leading order term constant, hypothesizing a "best packer" behavior for typical lattices in high dimensions and the other with leading $\ln(d)$.[11] For the first we obtain

$$\langle e\rangle = (0.58 \pm 0.04) - \frac{\ln(d)}{d}(0.9 \pm 1.0) - (0.8 \pm 0.6)d^{-1}. \tag{37}$$

The constant term is suggestively close to the Torquato-Stillinger bound, and, within the associated error, it is below the Minkowsky bound $\ln(2) = 0.69$. However, an equally good fit can be obtained by assuming that the leading term is growing logarithmically:

$$\langle e\rangle = (0.066 \pm 0.04)\ln(d) + (0.27 \pm 0.04) - (1.4 \pm 0.2)d^{-1}, \tag{38}$$

although the coefficient of the logarithm is well below the value 0.5 of the A_d and D_d families (typical lattices are much denser than these examples). Both fits are equally good; as can be seen from Fig. 11, the resolution of the two can occur only for $d \gg 40$.

The main effect of isometry on distribution of energies $\mathcal{P}(e)$ is to suppress low energy spikes (see Fig. 9) associated with dense lattices which are relatively often visited in these dimensions by a random walk, and shift the weight to the universal bell-like feature which dominates the distribution $\mathcal{P}_d(e)$ in high dimensions as presented in Fig. 12. As for the distribution of kissing numbers Z switching on the isometry testing kills the large-Z tail of the distribution and concentrates the weight around small values of Z of order $d(d+1)$ (recall that this is the lower bound on kissing number for perfect lattices). These facts indicate that in high dimensions typical perfect lattices have relatively high energy (but still lower than A_d and D_d) and small kissing numbers, of order $d(d+1)$. If we define rescaled variable $x = (e - \langle e\rangle_d)/\sigma_e$ we expect the probability distribution functions of x to collapse on some master curve with mild dependence on d:

$$\mathcal{P}_d(x) \propto \mathcal{P}_d\left(\frac{e - \langle e\rangle}{\sigma_e}\right).$$

Indeed, after rescaling a master curve is emerging as shown in Fig. 13 though the collapse is not perfect: The case $d = 12$ is special with a quite different shape as compared to other dimensions as highlighted in Fig. 13. All the distributions are skewed to the left, i.e., towards denser lattices, although this is hard to spot in Fig. 13 while this is clearly so for $d = 12$. These features become more pronounced if one studies $g_d(x) = -\ln \mathcal{P}_d(x)$, shown in Fig. 14: The generic skewness to the left (towards the denser lattices) becomes clear. For all dimensions studied except $d = 12$ the central part of $g_d(x)$ can be well fitted with a Gaussian

$$-\ln \mathcal{P}_d(x \sim 0) \sim 0.85 + \frac{x^2}{1.8};$$

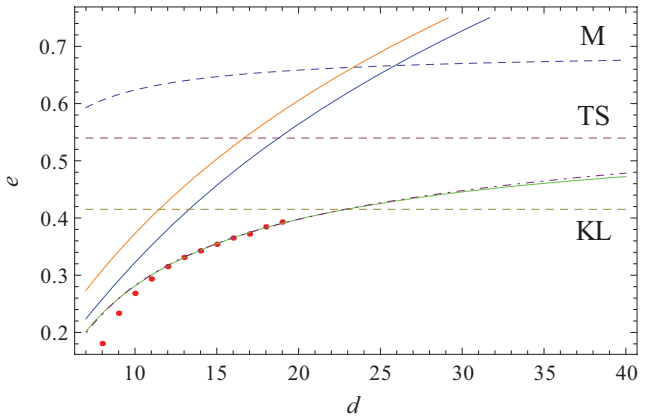

FIG. 11. (Color online) Average energy $\langle e\rangle = -\frac{1}{d}\langle \ln \phi\rangle$ of a random walk as a function of dimension ($d = 8 - 19$) (red dots) compared to energy of A_d and D_d lattices [yellow/top solid and blue/next to the top solid continuous lines; see Eq. (31)]. The dashed curves are the leading asymptotics of the *Minkowksy* (M, top), *Torquato-Stillinger* (TS, middle) and *Kabatiansky-Levenstein* (KL, bottom) bounds. The Minkowksy and Torquato-Stillinger are upper bounds, while the Kabatiansky-Levenstein bound is a lower bound on the energy of the best packing. The green/lowest solid and purple/dot-dashed lines are the two fits (37) and (38).

[11]We use eight points between $d = 12$ and 19; no sensible differences are obtained including less points in this range.

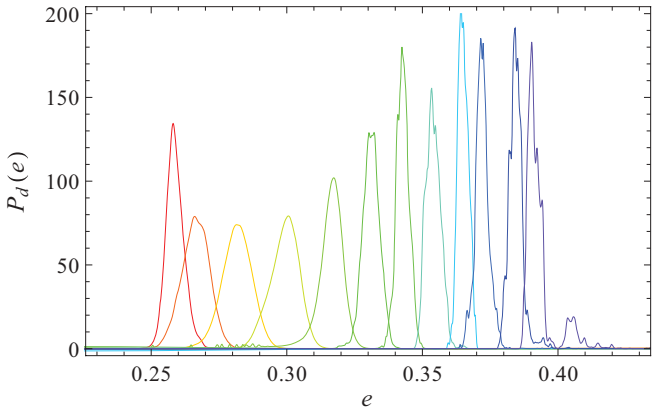

FIG. 12. (Color online) Probability distributions $\mathcal{P}_d$ of energy e for $d = 8$–$10, 12$–19; color/peak goes from red/left ($d = 8$) to violet/right ($d = 19$). As dimension increases averages increase and peaks shift to the right.

the value of the coefficient of x^2 being slightly larger than (but still consistent with) $1/2$ reflects the skewness of the distribution. The skewness appears only for larger values of x which are noisy because we do not have enough statistics to probe them accurately.

We now study the statistics of kissing number. For a typical perfect lattice the kissing number is of order d^2, i.e., like for A_d or D_d, and of the same order of magnitude as the lower bound $d(d+1)$. To highlight this point we normalized $\langle z \rangle$ by $d(d+1)$, the minimal possible kissing number which gave a curve shown in Fig. 16. Thus a typical perfect lattice is similar to A_d or D_d in kissing numbers but has a lower energy or higher packing fraction. As we see from Figs. 15 and 16 the kissing number fluctuates much stronger than energy, and the only conclusion we can make from the plots is that the distributions concentrate around their means just like it happens with energy. Combining this observation together with behavior of average energy we see that in high dimensions the Voronoi graph is dominated by lattices which have properties similar to A_d and D_d.

C. Random walk with $\beta > 0$

As the dimension of space is increased beyond $d = 13$ we are no longer able to recover the densest known lattice packing with a plain random walk, at least for the number of steps we have tried (from a few hundred thousands to a few millions, depending on dimension). Given a fast growth of the number

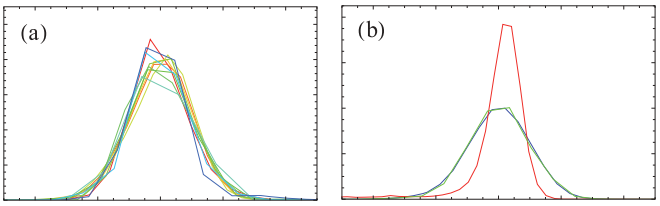

FIG. 13. (Color online) (a) Probability distributions $\mathcal{P}(x)$ vs x for $d = 8$–$10, 13$–17; color goes from red for $d = 8$ to magenta for $d = 19$. We have used exact distribution for $d = 8$ for convenience and skipped $d = 12$. (b) Comparison of distributions $\mathcal{P}_d(x)$ for $d = 10, 12, 13$. The case $d = 12$ (red, the highest peaked curve) is very distinct from neighboring dimensions shown here for comparison.

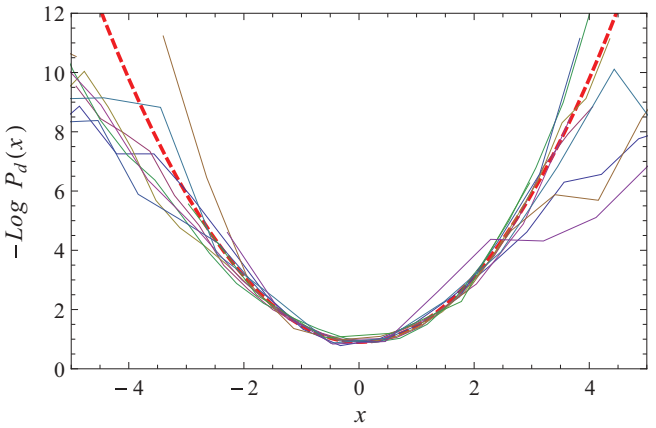

FIG. 14. (Color online) Gaussian fit (red dashed curve) to the central part of the probability distributions $\mathcal{P}_d(x)$ for $d = 8$–$11, 13$–19.

of perfect forms with dimension, one would likely have to sample random walks of size comparable to the number of perfect forms to see the densest lattices, something that is out of reach already for moderate dimensions $d \sim 13$–14.

We therefore introduced a procedure which biases the walk towards denser lattices. We employed the standard Metropolis-like rule with fictitious temperature β described in Sec. V which favors denser lattices. Namely, we generate a neighbor Q' of the lattice Q and compute its packing fraction $\phi(Q')$ and from this its energy $e(Q')$. If $e(Q') \leqslant e(Q)$, we accept the move, and if $e(Q') > e(Q)$, we accept the move only with probability $\exp[-\beta(e(Q') - e(Q))]$.

This allowed us to recover consistently the densest (known) lattice packings up to $d = 17$ and to get very close to the best known lattices in $d = 18, 19$, where we start seeing some complex landscape behavior. We managed to get the best known packing in these dimensions too but in a much less consistent fashion.

Again we are looking at distributions and moments, average, and standard deviation of energy and kissing number. We saw for a plain random walk which corresponds to $\beta = 0$ that $E(d) = \langle e \rangle$ is a smooth curve as a function of dimension. As the temperature is lowered $E_\beta(d)$ curves become more singular

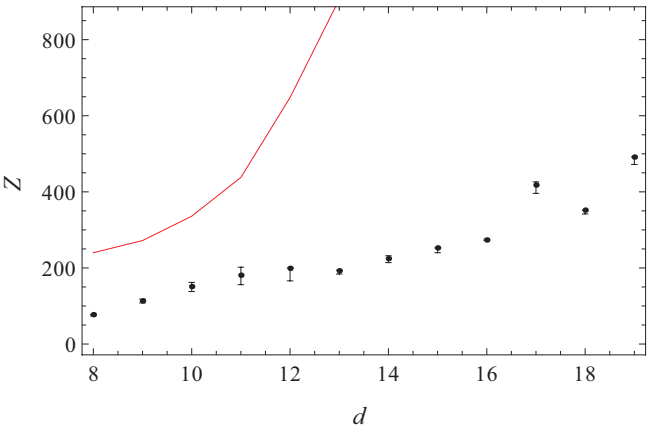

FIG. 15. (Color online) Average kissing number for $d = 8$–$10, 12$–19 (black dots). The red (top) curve is the best known kissing numbers in corresponding dimensions.

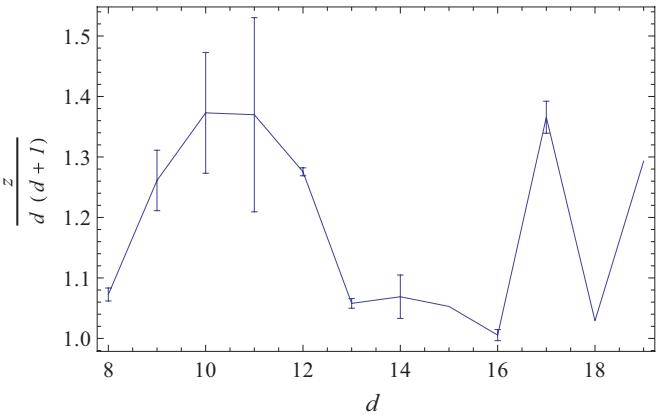

FIG. 16. (Color online) Average kissing number normalized by $d(d+1)$ for $d = 8$–19. Error bars correspond to first and third quartiles (these are zero for $d = 18, 19$). Despite strong fluctuations the value of normalized kissing numbers is of order 1.

reflecting the peculiarities of any given dimension (Fig. 17): It is well known that the nature of dense sphere packings varies greatly as a function of dimension, one of the factors that makes the problem of sphere packing so complicated. Up to $d = 11$ changing the temperature immediately affects the range of energies probed by the random walk: The lower the temperature the lower the energy and $E(\beta) = \langle e \rangle_\beta$ is essentially an exponentially decaying function of β (Fig. 18). Starting from $d = 12$ and up the pattern of $E(\beta)$ changes qualitatively: A plateau emerges at small β where the probed energy is almost insensitive to variations of temperature and is roughly equal to the energy of $\beta = 0$ random walk (see Fig. 19). As the inverse temperature β is increased there is a crossover to a lower value of energy. The value $E(\beta)$ for large β is approximately equal to the ground state energy, again almost insensitive to variation of β. Furthermore, sufficiently close to the crossover we observe a strong run to run fluctuations of values of $\langle e \rangle_\beta$, a phenomenon which is reminiscent of a glassy free energy landscape [28]. Such behavior suggests a phase transition as a function of β, as

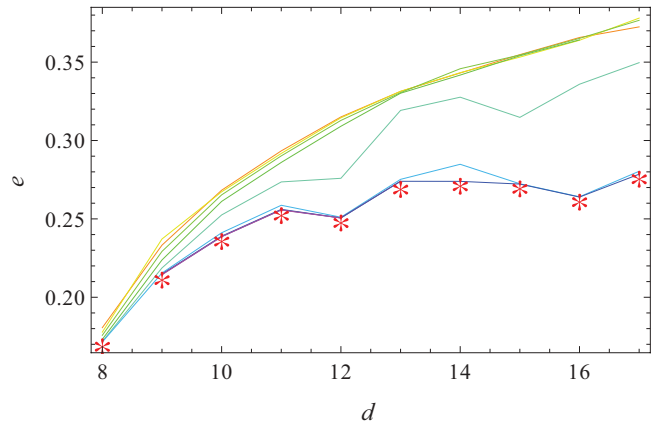

FIG. 17. (Color online) (Top) Average energy $\langle e \rangle = -\frac{1}{d}\langle \ln \phi \rangle$ of a biased random walk as a function of dimension $d = 8$–17: inverse temperature β goes from 0 (red/higher curves) to 5 (violet/lower curves); (red) asterisks mark the best known lattice packings. As the temperature is decreased, details of the scenarios in finite dimensions become relevant.

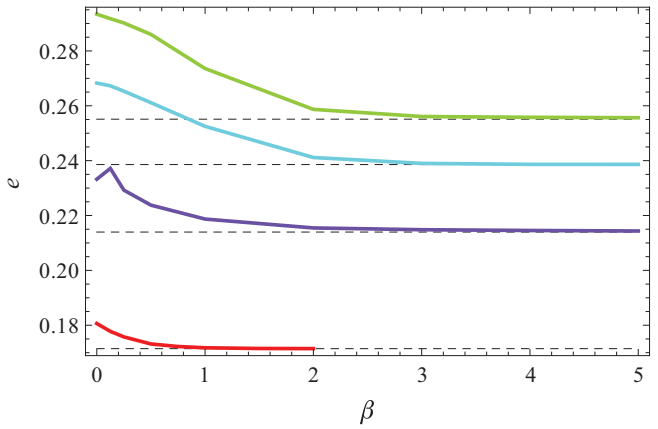

FIG. 18. (Color online) Average energy $\langle e \rangle = -\frac{1}{d}\langle \ln \phi \rangle$ of a biased random walk as a function of temperature for dimensions $d = 8$–11 (colors go from red to green, bottom curve is $d = 8$, top curve is $d = 11$); dashed lines are the best known energies in corresponding dimensions.

$d \to \infty$: As the temperature is lowered one leaves a *universal* phase dominated by typical perfect lattices and enters a phase where lattices with low energies dominate the biased random walks. To test this assumption we define $\beta_c(d)$ as a solution to $E_d(\beta_c) = E_c(d) = [E_d(0) + E_d(\infty)]/2$. As usual $E_d(\infty)$ should read as $E_d(\beta_1)$ for some sufficiently large β_1. The crossover width is defined as $\beta_<(d) - \beta_>(d)$ where

$$\Delta_d = \frac{E_d(0) - E_d(\infty)}{2},$$

$$E_<(d) = E_d(\beta_<) = E_d(\infty) + \frac{3}{4}\Delta_d = \frac{3}{4}E_d(0) - \frac{1}{4}E_d(\infty),$$

$$E_>(d) = E_d(\beta_>) = E_d(\infty) + \frac{1}{4}\Delta_d = \frac{1}{4}E_d(0) - \frac{3}{4}E_d(\infty).$$

The choice of factors 1/4 and 3/4 is not important, and they can be replaced by other number. If there is indeed a phase transition, then $W = (\beta_> - \beta_<)/\beta_c$ should converge to a constant value as $d \to \infty$. Figure 20 shows dependence of W on dimension. One observes, indeed, a tendency to

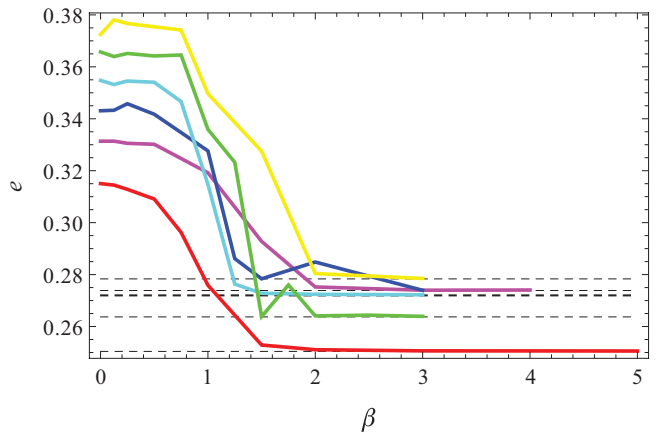

FIG. 19. (Color online) Average energy $\langle e \rangle = -\frac{1}{d}\langle \ln \varphi \rangle$ of a biased random walk as a function of temperature for dimensions $d = 12$–17 (colors go from yellow to red, bottom curve is $d = 12$, top curve is $d = 17$).

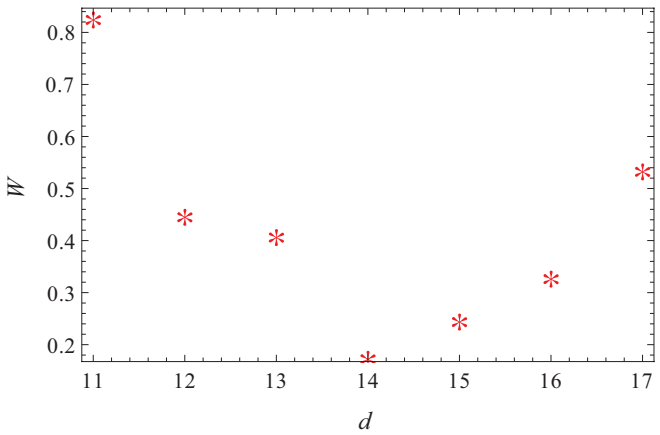

FIG. 20. (Color online) $W = (E_> - E_<)/E_c$ as function of dimension $d = 8$–18.

convergence to a constant value of $O(1)$ (although with noticeable oscillations around it). We attribute the increase for $d > 17$ to the glassy nature of the energy landscape of perfect lattices: These are exactly the dimension where the simple Monte Carlo approach starts experiencing problems finding the best packer. The $d = 18$ is intermediate between $d < 18$ and 19.

The situation seems to change qualitatively in $d = 18$ and 19: For mildly low temperature one has to increase drastically running time (as compared to $d < 18$) in order to reach the best known packings. For very low temperatures, $\beta \sim 3$–5 for $d = 18,19$, the Monte Carlo routine gets stuck around some relatively dense lattices and is never able to recover the densest lattice, or even approach it within the accuracy achieved in smaller dimensions. Typical energies reached by Monte Carlo are of order $e \sim 0.35$–0.36 for $\beta \lesssim 5$. This is to be compared to the ground state $e = 0.29$ corresponding to lattice Λ_{19}. It is then crucial to study higher dimensions in order to understand whether this behavior is a peculiarity of $d = 18,19$ or if it is a generic trend establishing in high dimensions. However, we are unfortunately currently unable to investigate dimensions higher than 19, but we hope to be able to do so in the future.

VII. DIAMETER OF THE VORONOI GRAPH

An interesting question is the number of perfect forms as a function of dimension d. The exact numbers for $d < 9$ and the estimate in $d = 9$ suggest a very steep, perhaps superexponential law which would make the full enumeration impossible beyond $d \sim 11$. We conjecture that the number of perfect lattices should grow as $\mathcal{N}_d \sim \exp(A\, d^2)$ for an appropriate constant A for large d. This conjecture is natural in the framework of statistical mechanics as the number of degrees of freedom is $O(d^2)$, and so should be the "entropy" of the system.

Looking at the distribution of the connectivities we can moreover conjecture that the Voronoi graph is a scale-free random graph, at least for a range of connectivities and for large d. For scale-free networks an estimate of number of vertices as a function of connectivities c of the vertices of the graph is [36]

$$\frac{\ln \mathcal{N}_d}{\langle \ln c \rangle} \simeq \mathrm{Diam}(\mathcal{G}_d). \tag{39}$$

Here $\mathrm{Diam}(\mathcal{G}_d)$ is diameter of the graph: the longest among the shortest paths between any pair of vertices.

We have estimated the diameter of the Voronoi graph $\mathcal{G}_d$ using the information on the graph provided by the random walk. This contains partial information and serves just as an order of magnitude consideration, so we must consider the dependence on the size of the sample. This computation becomes increasingly harder with growing d and, we have restricted this study to $d \leqslant 11$.

If the distribution of the connectivity is indeed scale free with fixed exponent 2.6, we find that

$$\langle \ln c \rangle = \frac{1}{2.6 - 1} = 0.62. \tag{40}$$

We find a reasonable agreement with numerical estimates of $\langle \ln c \rangle$: 1.274, 0.954, 0.771, 0.7 for $d = 8,9,10,11$, respectively. The excess of values of $\langle \ln c \rangle_d$ with respect to conjectured value 0.62 is due to the fact that we sample many well-connected, dense lattices while not visiting many lattices with low connectivity. Therefore the logarithm of the size of the graph and the diameter should be proportional as

$$\ln \mathcal{N}_d \simeq 0.62\ \mathrm{Diam}(\mathcal{G}_d). \tag{41}$$

We can then test if our hypotheses on the connectivity, the number of forms, and size of the graph fit well together. We find graph diameters 3, 6, 13, 32, and 131 for $d = 7,8,9,10,11$, respectively. Remark that the exact diameter is 3 and 4 in $d = 7$ and 8, respectively. The growth is clearly faster than linear as shown in Fig. 21 and is consistent with the hypothesis of scale-free Voronoi graph. The quadratic fit for $\mathrm{Diam}(\mathcal{G}_d)$ based on data for $d = 7 - 10$ reads as

$$\mathrm{Diam}(\mathcal{G}_d) = 217.6 - 58.6\, d + 4\, d^2.$$

However, with the actual data we cannot find the precise scaling. Although the exponential fit looks more accurate than the quadratic in Fig. 21, we know that there are many forms in $d = 11$ which were not visited by a random walk. Their addition to the graph would reduce the diameter and perhaps smear the seemingly exponential growth. More data

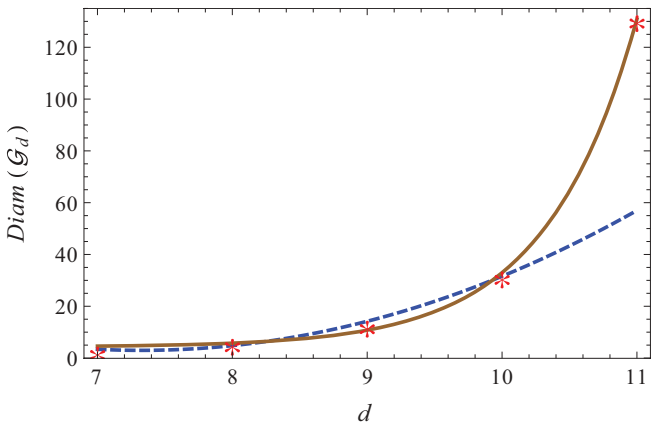

FIG. 21. (Color online) (Red) asterisks: estimate of diameter of the Voronoi graph as function of dimension. Blue/dashed and brown/solid curves are quadratic and exponential fits, respectively, provided here as guides for the eye.

Input: Voronoi domain $\mathcal{V}(Q)$
Pick an inequality at random
Saturate the inequality, i.e. replace it with equality
Make a random Gaussian cost function f as before
Solve linear program to get an extreme ray
Output: Random extreme ray R

FIG. 22. Algorithm for uniformized random extreme ray generation.

are required to resolve this issue, and we leave the resolution of this problem for future work.

VIII. TRYING TO UNIFORMIZE THE CHOICE OF A NEIGHBOR

As we have already mentioned above, the randomization of the Voronoi algorithm is not unique: Different cost functions (26) produce slightly different results. We have considered a number of functions, targeting uniformization, i.e., trying to make sampling of rays or neighbors more uniform, more like it is for full enumeration. In all cases we observed a bias towards denser forms with higher kissing numbers, which we try to reduce. In particular we constructed a "uniformized" cost function as shown in Fig. 22 [recall that we have a n-dimensional polyhedron, $n = d(d+1)/2$ here, defined by a set of inequalities, the number of inequalities $\mathcal{N} \geqslant n$]. This construction is inspired by the remark that a purely random cost function generates rays weighted with areas of facets adjacent to that ray, and it also favors forms that have higher connectivity, i.e., number of neighbors. This is an advantage if one is interested in denser forms. However, if one is studying properties of the Voronoi graph it might be preferable to make the outcome of neighbor generation more uniform.

The above construction tries to give facets a more uniform weights. Comparison of numerical results for random and uniform cost functions is presented in Fig. 23, which shows distributions of the kissing number and energy in $d = 8$. There is no significant difference of distributions between the *random* and *uniformized* cost function. However, the uniformized cost function is advantageous over the random function if one is interested in the properties of the Voronoi graph: Typically it yields more nonisometric forms than the pure random function for equal number of runs. We have performed this comparison for $d = 8$–12, and results are summarized in the table below (where the Fraction column is a ratio $\mathcal{N}_u/\mathcal{N}_r$ of number of forms found $\mathcal{N}_r$ and $\mathcal{N}_u$ with *random* and *uniformized* cost functions, respectively):

Dim.	Steps	Random	Uniformized	Fraction
8	2×10^6	1793	2955	1.648
8	4×10^6	2529	3963	1.567
10	10^6	331 065	434 317	1.312
11	10^6	744 282	825 695	1.109

The difference between the two cost functions is decreasing rapidly as dimensionality is increased. We believe that these strategies are better suited for lower dimensions $d \lesssim 12$ where isometry is important.

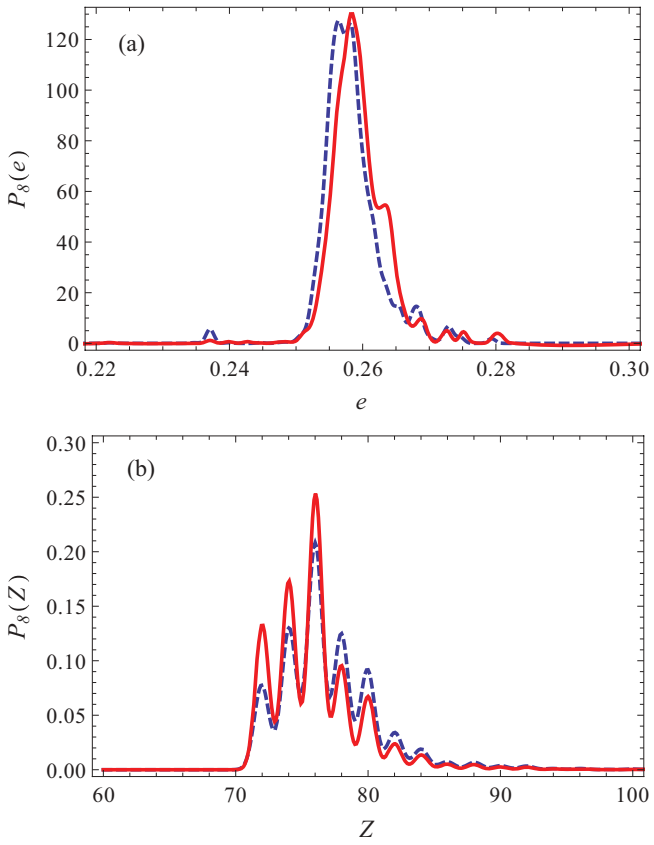

FIG. 23. (a) Distribution of energies. (b) Distributions of kissing numbers. Blue(dashed) and red(solid) curves are generated by random walks in $d = 8$ with *random* and *uniformized* cost functions.

IX. EXTENSION TO PERIODIC SETS

Before concluding let us describe a possible extension of our approach to lattices with many particles per unit cell, which we refer to as periodic sets throughout this section. Such an extension is possible but has a number of limitations which make the problem more difficult than the Bravais lattice version.

The generalization of the Voronoi algorithm to periodic sets was introduced by Schürmann [17]. An m-periodic set is defined by a quadratic form which describes how a unit cell is translated in space and a set of m real vectors (*translational part*) that defines the positions of m particles inside the cell. It is then possible to extend the Voronoi theory presented in Sec. II and introduce m-perfect and m-eutactic lattices; *m-extreme* lattices are defined as local maxima of a packing fraction of m-periodic sets, just like in the Bravais case. There is as well an analog of the Ryshkov polyhedron.

It is at this point that a crucial difference appears which makes the problem more complicated than the lattice one. In general not all extreme lattices are m-perfect and m-eutactic: There exist lattices which are extreme, but not perfect. An example is provided by *fluid diamond packings* [1] where a fraction of spheres can be moved around freely without changing the packing fraction. Furthermore the Voronoi graph no longer exists: The method provides only a local direction in which packing fraction is increasing. Potentially this allows

one to design an algorithm that starts with a periodic set and ends up at an m-perfect lattice [17]. On the other hand, the extension to many particles in a unit cell highlights the importance of perfect, strongly eutactic lattices since one can prove that they are *extreme* [29], that is, they are extreme among lattices with any number of particles per unit cell.

These limitations are lifted if one fixes translational part and replaces *real* vectors in the definition of a periodic set by their *rational* approximations [17]. Under this assumption, all the features of the Voronoi theory are recovered. Yet the complexity is increasing too: The computation of the shortest vectors of such periodic set is more involved.

X. COMPARISON WITH OTHER ALGORITHMS FOR GENERATION OF DENSE PACKINGS

It is instructive to compare the performance and the range of applicability of our method to other algorithms devised to generate dense packings [37–40]. The main difference with respect to these other approaches is that they perform searches and construct dense packings in an iterative manner from some initial guess imposing the *no overlap* constraints. We sample lattices from a large but finite set of perfect lattices which contains the densest lattice by construction and optimize the sampling procedure, while consequtive lattices are not necessarily close or similar or denser *a priori*. The advantage of the algorithms [39,40] is their universality, as they can be adapted to problems of packing other convex nonspherical bodies, like tetrahedra, while the Voronoi theory is hardly if at all extendable to cover these cases. On the other hand we expect to be able to study higher dimensions than other methods could probably handle.[12]

XI. CONCLUSIONS AND FURTHER DIRECTIONS

We have suggested a new approach to the lattice sphere packing problem based on randomization of the exact Voronoi algorithm. Previous works used complete enumeration that becomes computationally unfeasible beyond $d \sim 10$–11 (see, however, Refs. [33,41–43]). We have developed an implementation of our algorithm that allowed us to study dimensions from 8 to 19 and we foresee its application for studying perfect lattices up to $d = 40$ at least (beyond that, technical problems with the implementation of the algorithm become conceptual problems).

We have studied statistical properties of the sets of perfect lattices generated by our algorithm, both typical and extreme values focusing on two quantities: energy, which we define as proportional to the logarithm of the packing fraction, and the kissing number. For all dimensions except $d = 19$ we were able to retrieve the best known packings starting from A_d or D_d lattices either using a simple random walk for $d \leqslant 12$ or biasing the random walk with temperature for $d > 12$. In $d = 19$ we had to restart the walk many times in order to hit the best packer: The random walk was always getting stuck in some higher-energy lattice, a phenomenon which is reminiscent of a glassy free energy landscape. The change of the average energy with temperature suggests the existence of a sharp phase transition as $d \to \infty$, although we cannot make a further argument on this topic, due to the large dimension-dependent fluctuations as the energy is lowered. We do not exclude that we will be able to say more on this topic in future work.

TABLE V. Fraction of eutactic and strongly eutactic discovered by random walks in $d = 8$–19.

Dimension	Fraction of eutactic lattices
8	0.2258
9	0.2351
10	0.3531
11	0.3246
12	0.1337
13	5.110e-03
14	3.000e-04
15	1.300e-04
16	8.000e-05
17	6.000e-05
18	1.250e-05
19	1.500e-05

We also found that the typical values tend to have much smoother behavior, and this allowed us to propose two possible scenarios for the large d behavior of the packing fraction of the typical perfect lattices. In one case we obtain an exponential decay of the packing fraction whose leading order improves upon the Minkowsky bound

$$\phi \sim 2^{-(0.84\pm0.06)d}, \tag{42}$$

while in the second case we have a faster, factorial-like decay

$$\phi \sim d^{-(0.06\pm0.04)d}, \tag{43}$$

however, with an unnaturally small exponent. A separation of these two behaviors would need investigation of lattices in dimensions 40 and higher.

Higher dimensions are also accessible and will require mostly technical rather than conceptual modifications in the code, at least for $d \leqslant 40$. Getting beyond $d = 24$ is important since dimensions below 24 are dominated by the Leech lattice Λ_{24}, and all the densest lattices in these cases are cross sections of Λ_{24}.

Other possible applications of our work include a test of the "decorrelation principle" in Ref. [6], by studying the two-particle correlation functions of typical perfect lattices, and a systematic study of the *perfect and eutactic* lattices, which are the true local minima of the energy for the purpose of unveiling a glassy structure of the energy landscape. Checking for eutaxy is quite straightforward, after a set of perfect lattices has been generated, but we found that this requires a much larger statistics than that used in our paper since the rejection rate is quite large: As the dimension of space is increased the fraction of (at least) eutactic lattices discovered by a plain random walk drops rapidly as illustrated in Table V. If one biases the walk with temperature the numbers increase, but they are still low, and we have not tested whether the increase

[12]The algorithm of Ref. [39] reproduced the densest packings up to $d = 14$ with very small running time (6s for $d = 14$). It would be interesting to understand how its performance scales with dimension.

is due to different lattices or isometric copies of few lattices. Therefore we leave this for future work.

Finally, the randomization procedure we have introduced could also be applied to other optimization problems like the lattice covering problem [17], where one searches for the most economical way of covering a space with spheres of equal size. Another possible activity along the same direction is to adapt our randomization procedure to the algorithm generating all eutactic lattices in a given dimension [30].

As we have indicated, finding extreme rays of the Voronoi domain $\mathcal{V}$ is a particular case of a general *polyhedral representation conversion problem* [34]. This is an important problem in *combinatorial optimization* and *computational geometry*. Although efficient algorithms exist for certain classes of polyhedra, its complexity in general is unknown [33,34], but all existing full conversion algorithms are exponential in the number of constraints that define a polyhedron [34]. In this wider context our randomization approach offers a possible work-around for optimization problems which require a solution of the representation conversion problem in order to find an optimum.

ACKNOWLEDGMENTS

We wish to thank A.Schürmann and G.Nebe for providing code for isometry testing. We are also indebted to S.Torquato, A. Kumar, and H. Cohn for many stimulating discussions. We would like to thank the developers of the PARI/GP [44] libraries for their quick response in fixing bugs. A.S. would like to thank the Center for Theoretical Physics at MIT where part of this work was completed.

APPENDIX A: SOME TECHNICAL DETAILS

The two main technical ingredients of the Voronoi algorithm are generation of a random extreme ray R of the Voronoi domain $\mathcal{V}(Q)$ and finding a neighbor Q' of a given lattice Q provided an extreme ray R.

Computing a random extreme ray has the same complexity as generating the Voronoi domain $\mathcal{V}(Q)$ and solving a linear program. We need to know shortest vectors of Q in order to build $\mathcal{V}(Q)$. Computing the shortest vectors of a lattice is an exponentially hard problem in d. However, good algorithms exist allowing computation to be carried out in reasonable time at least up to $d \sim 40$ [45,46]. The other source of complexity is the size of linear program, which is defined by a kissing number of Q (and hence scales exponentially in d for dense packings) and is limited by the ability of linear program (LP) solvers to cope with huge linear programs: Size of the LP becomes of order 10^{10} for the densest known lattices in $d \gtrsim 40$. Based on this observation we expect our method to work up to $d \sim 40$, at least in theory. It is also worth pointing out that it is straightforward to check if a given ray R is extreme [34].

Finding a neighbor $Q' = Q + \alpha R$ with $\alpha \in \mathbb{Q}$ proved to be a harder problem computationally, and it is this part of the problem that limited our data to $d < 20$. The value of α is rational [17,32], so that we can always choose Q' to be integral, and all perfect lattices then have integral representation. We use a modified binary search algorithm as defined by Schürmann [17] to compute neighbors of a lattice ($S^d_{>0}$ is set of all lattices) presented in Fig. 24. The idea behind this construction is very simple: The neighbor of Q is $Q' = Q + \alpha R$ with the smallest positive rational α such that $\lambda(Q) = \lambda(Q + \alpha R)$ and $\mathrm{Min}(Q + \alpha R) \not\subseteq \mathrm{Min}(Q)$.[13] In the first part of the algorithm presented in Fig. 24 upper and lower boundaries for α are defined. The second part of the algorithm is a modified binary search for value of α. The modification, an extra conditional in the assignment of u, is necessary to make the algorithm converge in a finite number of steps to an exact rational value of α.

Input: perfect form Q, extreme ray R
  while $Q + u\,R \notin S^d_{>0}$ and $\lambda(Q + u\,R) = \lambda(Q)$ **do**
    if $Q + u\,R \notin S^d_{>0}$ and $\lambda(Q + u\,R) = \lambda(Q)$ **then**
      $u \leftarrow (l + u)/2$
    else
      $(l, u) \leftarrow (u, 2\,u)$
    end if
  end while
  while $\mathrm{Min}(Q + l\,R) \subset \mathrm{Min}(Q)$ **do**
    $g \leftarrow (u + l)/2$
    if $\lambda(Q + g\,R) \geq \lambda(Q)$ **then**
      $l \leftarrow g$
    else
      $u \leftarrow \min\{(\lambda(Q) - Q[v])/R[v] | v \in \mathrm{Min}(Q + g\,R), R[v] < 0\} \cup \{g\}$
    end if
  end while
Output: $\alpha \leftarrow l$

FIG. 24. Modified binary search for neighbor Q' of a lattice Q given an extreme ray R.

APPENDIX B: RANDOM WALKS AND ISOMETRY CHECK

We have used two different approaches to perform checks for isometry of lattices. In the first approach we split the data generation into two steps: (1) Generate a random walk in space of lattices with no check for isometry and (2) run an isometry test on the trajectory of the random walk and generate an approximate Voronoi graph. After the first step one obtains a full trajectory of a random walk as list of lattices. The second step generates the graph by eliminating isometric copies of lattices by gluing together isometric elements of the list. This induces a relation of the neighborhood in the list and transforms the list into a graph.

The second possibility is to perform an isometry check and graph construction on the fly ($P \sim Q$ denotes isometric equivalence, and V and E are sets of vertices and edges of the graph G, respectively) as shown in Fig. 25.

Both algorithms terminate after a predefined number of steps has been done.

An algorithm to check whether two lattices are isometric was developed by W. Plesken and B. Souvignier in Ref. [27]. We adapted the original code of B. Souvignier to perform isometry testing.

[13]Note that self-loops are allowed, i.e. $\alpha \neq 0$ and $\mathrm{Min}(Q + \alpha R) = \mathrm{Min}(Q)$.

Input: perfect Q, graph $G = (V = \emptyset, E = \emptyset)$
loop
Random extreme ray $R \leftarrow Q$
Neighbor $Q' \leftarrow Q + \alpha R$
for $P \in G$ **do**
if $P \sim Q'$ **then**
$E \leftarrow E \cup (Q, P)$
else
$V \leftarrow V \cup Q'$
$E \leftarrow E \cup (Q', Q)$
end if
end for
end loop
Output: Voronoi graph G

FIG. 25. Algorithm that constructs an approximation to the Voronoi graph.

APPENDIX C: NAIVE RANDOM WALK

It is worth discussing performance of a straightforward approach that one might be tempted to follow. The Voronoi construction is elaborate and requires computational effort. *A priori* one might wonder if a simple *lattice random walk or Monte Carlo approach* [10] is preferable (maybe in higher dimensions?). The algorithm shown in Fig. 26 is extremely simple: One hopes to approach the best packer by small steps if the random walk is sufficiently biased towards denser lattices. When generating a move one has the option of either producing a new lattice A' which might or might not be an isometric copy of A. Acceptance probability p could be 1 (random walk) or, for example, the Metropolis rule (à la Monte Carlo).

An unbiased random walk (infinite temperature in our language) with moves that generate nonisometric lattices A'

Input: Lattice A
loop
$(*)$ $A' \leftarrow A$
Accept A' with some probability p
Goto $(*)$
end loop
Output: Dense lattice A

FIG. 26. Naive random walk.

gives an average packing fraction which is equal to the Minkovsky bound [9,10,47–49]. This is a rather strong result since the Minkovsky bound is nonconstructive and constructing a lattice in a given dimension satisfying the bound is yet an open problem. However, it is very hard to implement that type of updates in practice [9,10,47–50], and one has to rely on various approximations. In the case when one allows for any A' the performance of the algorithm is extremely poor: With the simple Gaussian measure for lattices [10] $\mathcal{P}(A) \sim \exp(-\gamma \operatorname{Tr} AA^t)$ we were able to recover the best packers in $d = 2,3$, although already in three dimensions we had to go to very low temperatures. The performance of the algorithm quickly deteriorates with dimension, and by $d = 10$ it is completely useless. The above mentioned variant of the algorithm where one samples only among the nonisometric lattices has similar performance when approximations are used. Finally it is worth mentioning that the lattices generated by such Markov chains are never perfect and are typically far from being such.

These negative results provide an extra motivation for studying perfect lattices and the Voronoi construction where much better performance is achieved.

[1] J. H. Conway and N. J. A. Sloane, *Sphere Packings, Lattices and Groups*, Vol. 290 (Springer, New York, 1999).
[2] C. Shannon, Bell Syst. Tech. J. **27**, 379 (1948).
[3] S. Torquato, *Random Heterogeneous Materials* (Springer, New York, 2005).
[4] L. Fejes Tóth, Math. Z. **46**, 83 (1940).
[5] T. Hales, Ann. Math. **162**, 1065 (2005).
[6] S. Torquato and F. H. Stillinger, Exp. Math. **15**, 307 (2006).
[7] C. Zachary and S. Torquato, J. Stat. Mech. (2011) P10017.
[8] A. Scardicchio, F. H. Stillinger, and S. Torquato, J. Math. Phys. **49**, 043301 (2008).
[9] C. Rogers, Proc. Lond. Math. Soc. **3**, 609 (1958).
[10] G. Parisi, J. Stat. Phys. **132**, 207 (2008).
[11] Y. Jin, P. Charbonneau, S. Meyer, C. Song, and F. Zamponi, Phys. Rev. E **82**, 051126 (2010).
[12] G. Parisi and F. Zamponi, J. Stat. Mech. (2006) P03017.
[13] G. Parisi and F. Zamponi, Rev. Mod. Phys. **82**, 789 (2010).
[14] H. Cohn and N. Elkies, Ann. Math. **157**, 689 (2003).
[15] H. Cohn and A. Kumar, Ann. Math. **170**, 1003 (2009).
[16] G. Voronoi, J. Reine. Angew. Math. **133**, 97 (1908).
[17] A. Schürmann, *Computational Geometry of Positive Definite Quadratic Forms: Polyhedral Reduction Theories, Algorithms, and Applications*, Vol. 48 (American Mathematical Society, Providence, RI, 2009).
[18] A. Ash, Can. J. Math **29**, 1040 (1977).
[19] J. Lagrange, Nouv. Mém. Acad. Berlin 265 (1773).
[20] C. Gauss, J. Reine. Angew. Math. **20**, 312 (1840).
[21] A. Korkin and E. Zolotarev, Math. Ann. **11**, 242 (1877).
[22] E. Barnes, Philos. Trans. R. Soc. Lond. A **249**, 461 (1957).
[23] D. Jaquet-Chiffelle, Ann. Inst. Fourier (Grenoble) **43**, 21 (1993).
[24] M. D. Sikirić, A. Schürmann, and F. Vallentin, Electron. Res. Announc. Am. Math. Soc **13**, 21 (2007).
[25] C. Riener, J. Theorie Nombres Bordeaux **18**, 677 (2006).
[26] A. Schürmann *et al.*, fma2.math.uni-magdeburg.de/~latgeo/ and http://www.geometrie.uni-rostock.de/.
[27] W. Plesken and B. Souvignier, J. Symb. Comput. **24**, 327 (1997).
[28] M. Mezard, G. Parisi, and M. Virasoro, *Spin Glass Theory and Beyond*, Vol. 9 (World Scientific, Singapore, 1987).
[29] A. Schürmann, Advances in Mathematics **225**, 2546 (2010).
[30] C. Batut, Math. Comput. **70**, 395 (2001).
[31] A. Bergé and J. Martinet, J. Lond. Math. Soc. **53**, 417 (1996).
[32] J. Martinet, *Perfect Lattices in Euclidean Spaces*, Vol. 327 (Springer, New York, 2003).
[33] D. Bremner, M. D. Sikirić, and A. Schürmann, CRM Proceedings & Lecture Notes, 45 (American Mathematical Society, Providence, RI, 2009).
[34] D. Avis, D. Bremner, and A. Deza, *Polyhedral Computation*, Vol. 48 (American Mathematical Society, Providence, RI, 2009).

[35] A. Lenstra, H. Lenstra, and L. Lovász, Math. Ann. **261**, 515 (1982).
[36] B. Bollobás and O. Riordan, Combinatorica **24**, 5 (2004).
[37] B. D. Lubachevsky and F. H. Stillinger, J. Stat. Phys. **60**, 561 (1990); B. D. Lubachevsky, F. H. Stillinger, and E. N. Pinson, *ibid.* **64**, 501 (1991).
[38] H. Cohn, A. Kumar, and A. Schürmann, Phys. Rev. E **80**, 061116 (2009).
[39] Y. Kallus, V. Elser, and S. Gravel, Phys. Rev. E **82**, 056707 (2010).
[40] S. Torquato and Y. Jiao, Phys. Rev. E **82**, 061302 (2010).
[41] M. D. Sikirić, A. Schürmann, and F. Vallentin, Math. Comput. **78**, 1713 (2009).
[42] M. D. Sikirić, A. Schürmann, and F. Vallentin, Discrete Comput. Geom. **44**, 904 (2010).
[43] T. Rehn and A. Schürmann, *Mathematical Sofware ICMS 2010*, Lecture Notes in Comput. Sci., Vol. 6327 (Springer, Berlin, 2010), pp. 295–298.
[44] The PARI Group, Bordeaux, PARI/GP, version 2.5.2 (2012), http://pari.math.u-bordeaux.fr/.
[45] U. Fincke and M. Pohst, Math. Comput. **44**, 463 (1985).
[46] H. Cohen, *A Course in Computational Algebraic Number Theory*, Vol. 138 (Springer, New York, 1993).
[47] C. A. Rogers, Acta Mathematica **94**, 249 (1955).
[48] C. A. Rogers, Proc. Lond. Math. Soc. **3**, 305 (1956).
[49] C. A. Rogers, *Packing and Covering*, Cambridge Mathematical Tracts, No. 54 (Cambridge University Press, Cambridge, 1964).
[50] C. Siegel, Ann. Math. **46**, 340 (1945).